FEATURE ARTICLE

Salting Benzenes†

Richard W. Gurney, Christine A. Mitchell,‡ Sihyun Ham, Loyd D. Bastin, and Bart Kahr*

Department of Chemistry, University of Washington, Box 351700, Seattle, Washington 98195-1700

Received: July 15, 1999; In Final Form: October 28, 1999

Simple salt crystals, such as potassium sulfate or barium acetate, were grown in the presence of a variety of aromatic molecules, especially aniline derivatives, bearing sulfonate or carboxylate substituents. We call this process salting, borrowing the term from Michl and co-workers who coined it in a related context (Kirkor, E.; Gebicki, J.; Phillips, D. R.; Michl, J. *J. Am. Chem. Soc*. **1986**, *108*, 7106−7107). Particular growth sectors of the resultant crystals were luminescent, and the emitted light was highly polarized indicating that the benzene derivatives were oriented inside of the salt lattices. These results are presented in the context of a generalization of single crystal matrix isolation; isomorphous matching of hosts and guests need not be a constraint. We show by polarization spectroscopy and magnetic resonance that different faces of the crystals will entrap molecules in different conformations otherwise separated by small energies in solution. Metastable triplet states are remarkably long-lived at room temperature in salt matrixes. The mechanisms of benzene derivative incorporation depend highly on secondary surface structures that are imaged by differential interference contrast microscopy. Luminescent molecules identify these features by lighting-up particular substructures and as such serve as probes of crystal growth mechanisms. We show how patterns of light in crystals are used to assign absolute growth directions. We conclude by arguing that the results herein can be extended to a limitless range of guests, while encouraging the use of salts as matrixes for the study of organic compounds.

I. Introduction

A. Salting. In 1986, Michl and co-workers introduced the term *salting* to describe the incorporation of neutral organic molecules such as benzene or naphthalene in microcrystalline alkali halide matrixes such as NaCl and KBr. In a furnace, they deposited salts concomitantly with volatile organics onto a cold window for subsequent spectroscopic analysis.[1] Aromatic guests tended to aggregate in the polycrystalline salts. On the other hand, individual molecules of quadricyclane, for example, were detected spectroscopically and could be manipulated photochemically once inside the salt matrix.[2,3]

Why salt organic molecules? We cannot provide a better justification than that of the inventors of this methodology who forecast that salted organic molecules might someday offer convenient room-temperature storage for reactive molecules. They continue: "It would permit low-temperature and high-temperature investigation of...molecules in a highly unusual and yet possibly quite well-defined environment, which may significantly alter their spectroscopic, photochemical, and oxidation−reduction behavior. It would permit examination of temperature-dependent properties of the isolated molecules, including the study of the equilibrium population of low-lying excited states, normally negligible at the low temperatures characteristic of ordinary matrix isolation conditions, and the study of unimolecular reactions with sizable activation barriers. It would permit probing of defects in the solid, such as color centers, through their interaction with the dopant. In a more general sense, the effects of the doping on the properties of the host solid, such as photoconductivity, dark conductivity, absorption, and spontaneous or stimulated emission, may be of even more interest than the effects of the host on the guest molecule".

Here, we illustrate a method for the matrix isolation of aromatic compounds in large, single, well-faceted, transparent, ionic crystals that only requires the evaporation of water. This work has evolved from studies in our laboratories over the past seven years of salts containing oriented organic dyes. These unusual mixed crystals, discarded curiosities from the nineteenth century, can form when functionalities on the organic guests are prearranged such that they match stereochemical features of the salt surfaces. Once bound, the chromophores are subsequently encapsulated in highly defined orientations within specific growth sectors.

B. Dyeing Crystals. The first dyed salt crystal, $Sr(NO_3)_2 \cdot 4H_2O$ colored with hematein, was prepared by Sénarmont in 1854 in his attempt to demonstrate artificial pleochroism.[4] Additional systems were subsequently introduced in the course of a variety of researches.[5] Unfortunately, these mixed crystals of salts and dyes have not been objects of systematic study since the 1930s, a time before conformational analysis and spectroscopies were sufficiently well developed to enable a comprehension of structure. Thus, dyed salts disappeared from the literature.[6]

† Dedicated to Professor J. Michael McBride on the occasion of his 60th birthday.

‡ Current address: Lilly Research Laboratories, Eli Lilly and Company, Indianapolis, IN 46285.

10.1021/jp992424p CCC: $19.00
Published on Web 01/15/2000

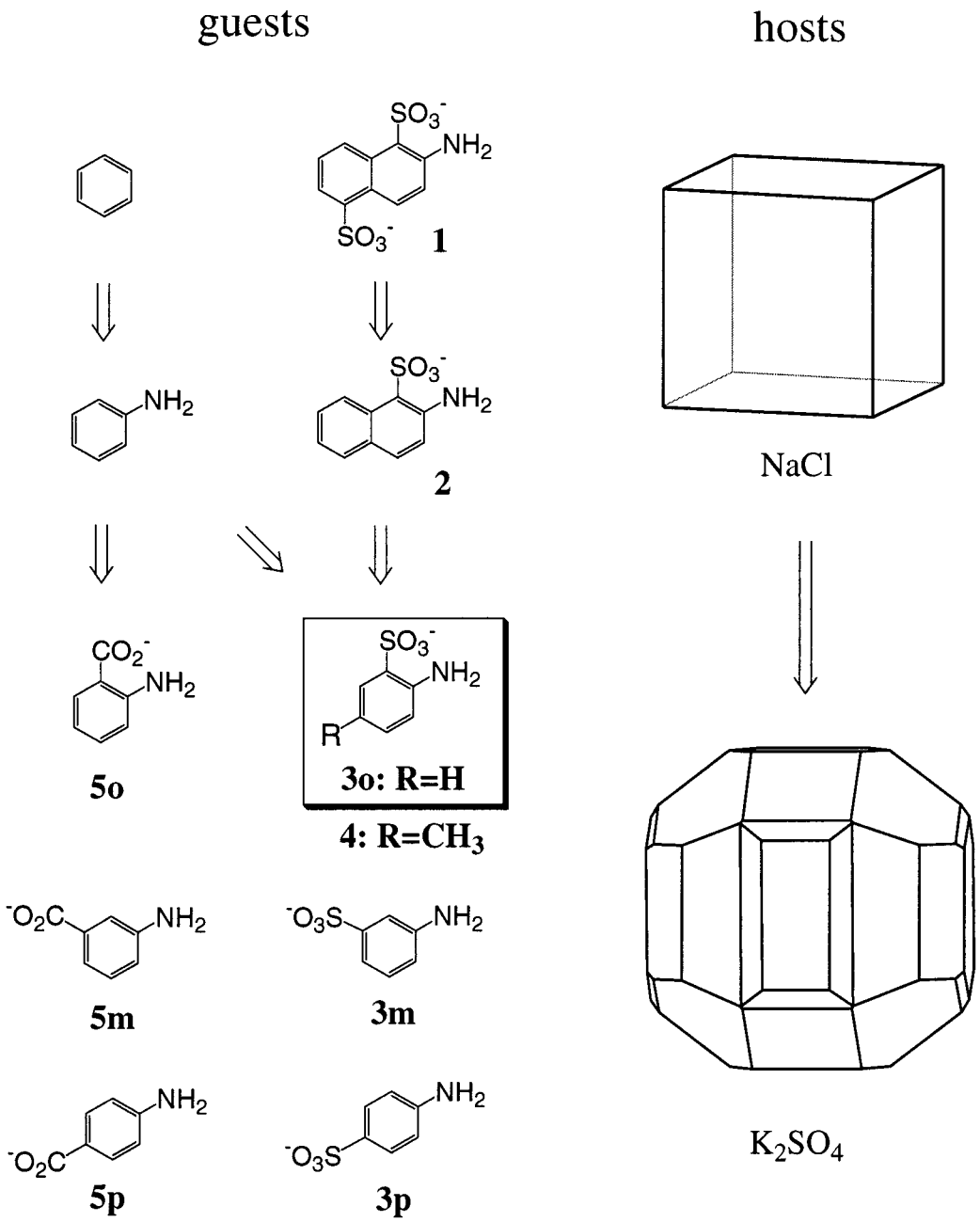

Figure 1. Evolution of guest and host.

In recent years we have attempted to revive the art and science of dyeing crystals, emphasizing simple salts as hosts.[7] We showed how structural studies of some historical K_2SO_4 dye inclusion crystals[8] were used in the design of new mixed crystals with prescribed functions such as lasing.[9] Enantioselective recognition was illustrated with KH_2PO_4.[10] We examined the internal texture of dyed crystals using X-ray topography[11] and the influence of ferroelectric phase transitions on dyes in Rochelle salt (sodium potassium tartrate).[12] We observed that acetate hosts, by limiting internal dynamics of included guests, obviated the collisional deactivation of metastable excited states (see section II. B.2).[13] We also examined organic hosts[14] and biological guest molecules with intrinsic chromophores.[15]

C. Choice of Chemical Systems. Benzene and NaCl, icons of organic and inorganic chemistry, respectively, are partners in the prototypical salted system. In our work, we have forfeited the simplicity of benzene in NaCl by relying on benzene derivatives in more complex ionic solids.[16] On the other hand, we now have the spectroscopic advantage of large single-crystal samples as opposed to polycrystals.

As a host, we began with K_2SO_4, whose crystals express 10 or more facets as opposed to NaCl which displays only {100}.[17] We observed {100}, {010}, {001}, {011}, {110}, {111}, {021}, {112}, {031}, and {130}. (Groth also reported {012} and {332}.) Compare the morphologies in Figure 1. These Miller indices refer to ratios determined by classical goniometry[18] (The corresponding axial lengths are $a = 5.772$ Å, $b = 10.072$ Å, $c = 7.483$ Å for *Pmcn*, No. 62.)[19] As such, potential guest molecules in solution have many more growing crystal surfaces with which to interact. Each crystallization in effect consists of 10 different experiments.

As guests, we chose aminobenzene sulfonates or carboxylates instead of D_{6h} benzene. The latter is water insoluble and its lowest energy electronic transitions, $^1B_{2u} \leftarrow {}^1A_{1g}$, $^1B_{1u} \leftarrow {}^1A_{1g}$, are forbidden by symmetry. To render benzenes optically detectable in small quantities we broke the symmetry of C_6H_6 by

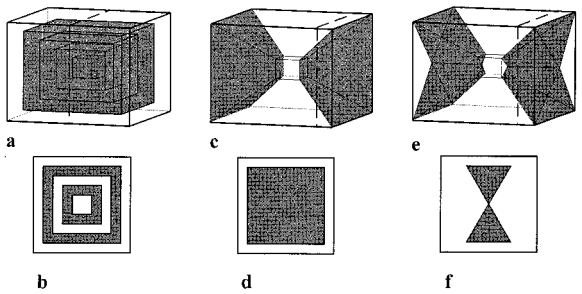

Figure 2. Idealizations of compositional zoning in an orthorhombic crystal grown from seed: (a,b) concentric, (c,d) intersectoral, and (e,f) intrasectoral zoning. (b,d,f) represent cross sections, indicated by broken lines in (a,c,e), respectively.

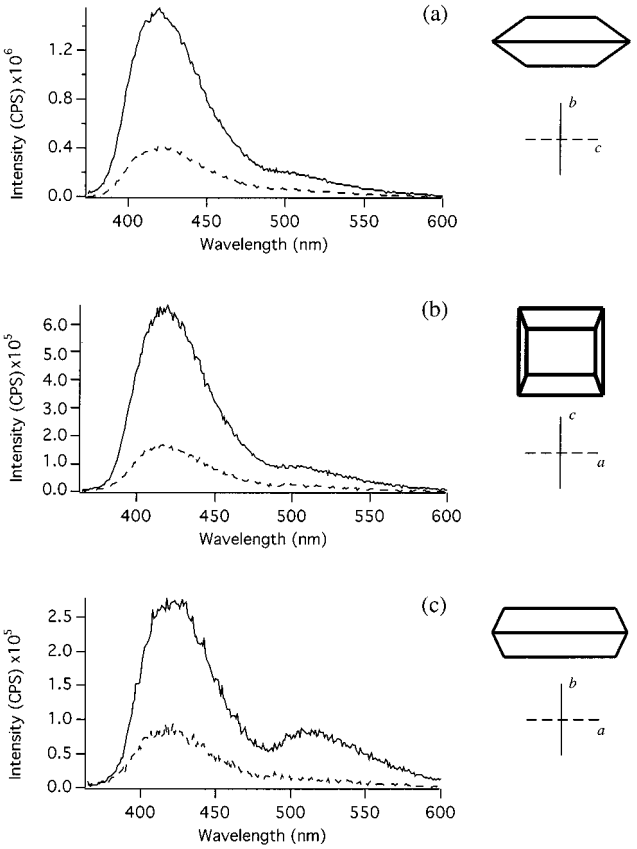

Figure 3. Luminescence spectra as a function of excitation (350 nm) polarization for thin sections of K_2SO_4/**1** single crystals with light incident along (a) the *a* axis, (b) the *b* axis, and (c) the *c* axis. Labeled axes below crystal figures indicate the orientation of the polarizer with respect to the crystal when recording the corresponding dashed and solid line spectra.

substituting the ring with an electron donating group ($-NH_2$). We then added an anionic group ($-SO_3^-$, $-COO^-$) for water solubilization, while providing an electrostatic driving force for mixed crystal growth.

The conceptual transformation of benzene to a benzene derivative, *ortho*-aminobenzenesulfonate (**3o**), amenable to analysis in a salt crystal (section II.A.2) is schematically shown in Figure 1. To separate history from implicit history, we have also included a "retrosynthetic" path to **3o** from 2-aminonaphthalene-1,5-disulfonate (**1**). Actually, we first observed room-temperature phosphorescence from K_2SO_4 grown in the presence of **1**, and in trying to determine the essential recognition elements we settled upon a more detailed analysis of **3o**.

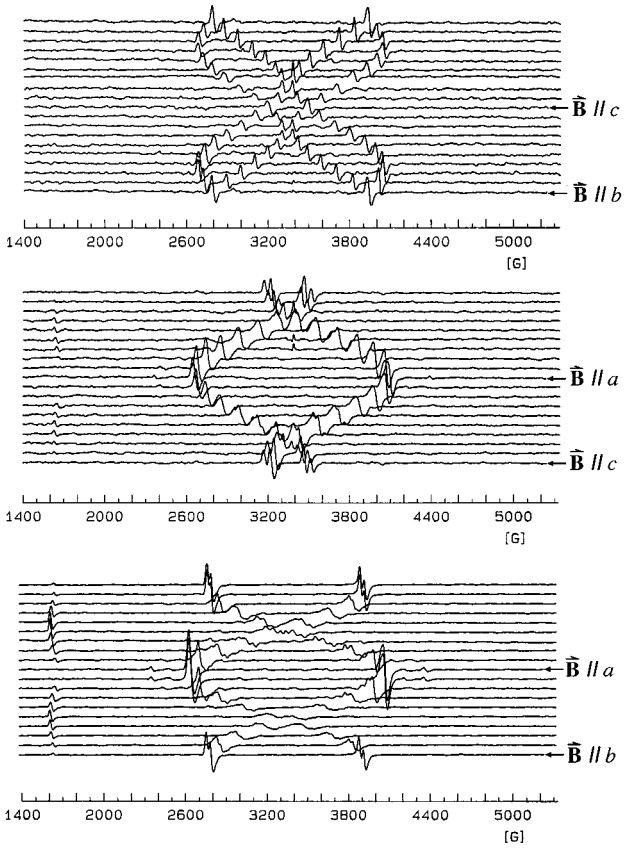

Figure 4. EPR rotation curves for photoexcited K_2SO_4/**1** single crystals.

II. Results and Discussion

A. Intersectoral Zoning. Guest molecules or ions interacting with growing host crystals must discriminate between faces that are not related to one another by symmetry. One consequence of this fact is that mixed crystals exhibiting more than one crystallographic facet will invariably display chemical zoning, different compositions from one growth sector to another. While there are countless examples of such phenomena in mineralogy,[20] as well as in synthetic crystals,[21] a molecular level understanding of such processes was first provided by Lahav, Leiserowitz, and their colleagues in a sweeping revision of the structure of solid solutions.[22] In our work, we explicitly call this phenomenon *intersectoral zoning*, to distinguish it from *temporal or concentric zoning*, compositional changes that come about as a function of crystal growth history, and from *intrasectoral zoning*, compositional heterogeneities occurring within individual growth sectors, Figure 2.

One of the many examples of intersectorally zoned crystals that we have studied in our laboratories is K_2SO_4 deposited from 10^{-3} M solutions of **1,** (from here on "K_2SO_4/**1**" notation will indicate single crystals of host/guest.) These crystals are remarkable in that they exhibit unusually long-lived green phosphorescence at room temperature in the {021} growth sectors that is perceived by the dark acclimated eye for up to 10 min.

1. Preserving Metastable States. Traditionally, the detection of phosphorescence from aromatic molecules has been restricted to analytes in frozen solutions. This limitation was overcome with the development of solid surface room-temperature phosphorescence (SSRTP), a simple method for observing phosphorescence from compounds deposited on solid surfaces.[23] Despite the growing use of SSRTP,[24] the luminophore and surface combinations that will produce measurable phospho-

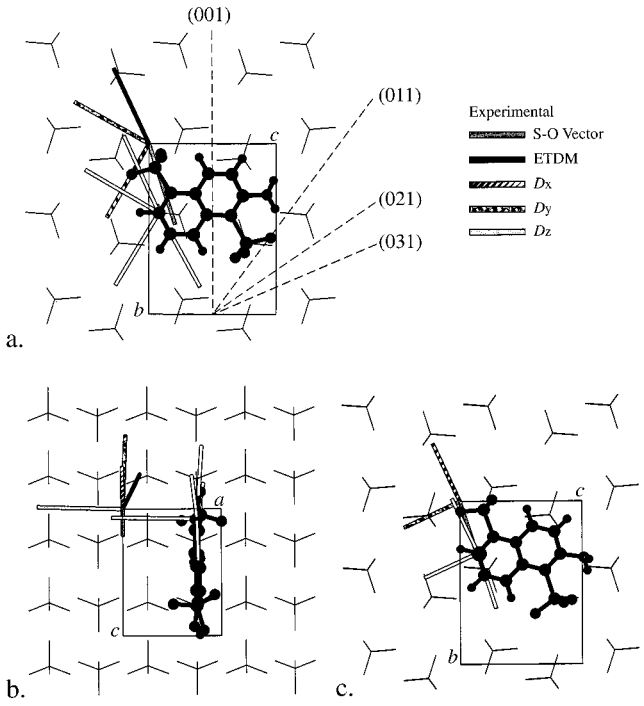

Figure 5. Models for the orientations of the major (a,b) and minor species (c) in K_2SO_4/**1** single crystals. K^+ ions have been omitted for clarity. Colorless bars represent calculated quantities for molecules. Black bars represent corresponding crystallographic quantities determined by experiment. Major species of **1** and **3o** have very similar orientations.

rescence quantum efficiencies cannot be predicted.[25] Given our observation of long-lived phosphorescence from mixed crystals, such as K_2SO_4/**1,** we were in a position to determine the nature of the host-guest interaction using optical and magnetic resonance spectroscopies, and thereby develop an understanding of the matrix's role in the preservation of the excited state.

The luminescence spectrum of K_2SO_4/**1** was distinguished from that in aqueous saturated K_2SO_4 solution by the phosphorescence peak at ~520 nm with a lifetime of 0.8 s (a minor longer-lived component must also have been present to account for the 10 min of visible phosphorescence). The luminescence intensity was measured as a function of excitation polarization (Figure 3) in each of the principal faces ($I_a/I_b = 0.29(1)$, $I_a/I_c = 0.28(1)$, $I_b/I_c = 4.4(1)$) and indicated an electronic transition dipole moment (ETDM) nearly in the *bc* plane, oriented toward *b*.

EPR spectra, of the triplet excited state of **1,** were recorded for photoexcited K_2SO_4/**1** rotated in the applied magnetic field around each of the principal axes (Figure 4). For rotations around *a* with the field applied between the *b* and *c* axes we observed two magnetically nonequivalent species, the expected behavior for one molecule in a triplet state on a general position in a crystal with *mmm* symmetry. The absence of magnetically nonequivalent pairs for rotations around *b* and *c* was the consequence of an accidental isochrony, indicating that one of the zero-field-splitting (ZFS) eigenvectors was parallel to the axis (Figure 5). **D** and **g** tensors were fit to the magnetic field positions:[26] **g** ($g_x = 2.001(3)$, $g_y = 1.998(3)$, $g_z = 1.995$ (3)) and **D** ($|D_x| = 0.0424$ (2), $|D_y| = 0.0018(2)$, $|D_z| = 0.0442$ (2) cm^{-1}; $|D| = 0.0663\ cm^{-1}$; $|E| = 0.0203\ cm^{-1}$). Given that the largest ZFS eigenvector of aromatic molecules is typically perpendicular to the mean molecular plane,[27] **1** likely lies in the *bc* plane.

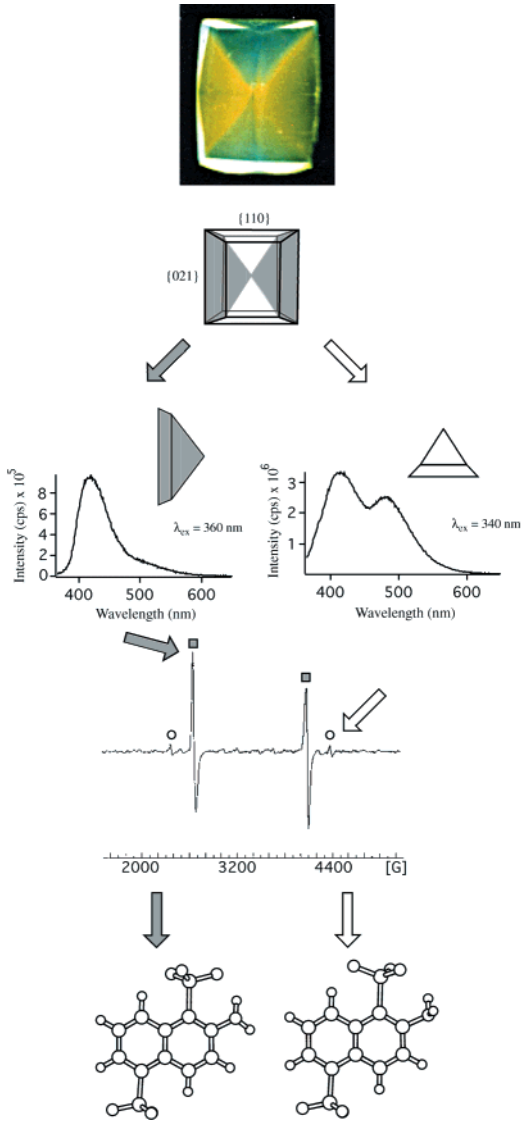

Figure 6. Summary of photophysical and magnetic differences between adjacent {021} and {110} growth sectors of K_2SO_4/**1** single crystals. From top to bottom: Photograph of crystal ($7 \times 5 \times 2\ mm^3$) showing two colors of phosphorescence and schematic representation of crystal habit, followed by luminescence spectra of the individual sectors, EPR spectra of whole crystals for magnetic field along the *a* direction, and the conformations to which the data are assigned with the $-NH_2$ group in and largely out of conjugation with the π-system. Major and minor EPR species marked with a square and a circle, respectively.

The orientation developed from optical spectroscopy and magnetic resonance by fitting the ETDM and the ZFS eigenvectors with corresponding quantities calculated using the INDO/S-CI method[28] and the point charge approximation,[29] respectively, suggested an inclusion mechanism where the sulfonate on the 1-position substituted for a sulfate on the (021) face with an S−O bond in the *bc* plane (Figure 5a,b).[30,31] Previous research from our laboratories has documented the importance of the electrostatic driving force of sulfonate-sulfate substitutions in dyeing K_2SO_4 crystals.[32] The sulfonate on the 5-position was considered superfluous, because 2-aminonaphthalene-1-sulfonate (**2**) formed mixed crystals with K_2SO_4 that showed similar optical and magnetic anisotropies ($|D| = 0.0766$(1) cm^{-1}, $|E| = 0.0202(1)\ cm^{-1}$), with eigenvectors oriented in precisely the same way with respect to the naphthalene frame. Given that crystals grown under identical conditions incorporated ~10 times more **2** than **1** (host:guest ratios of 5×10^4:1

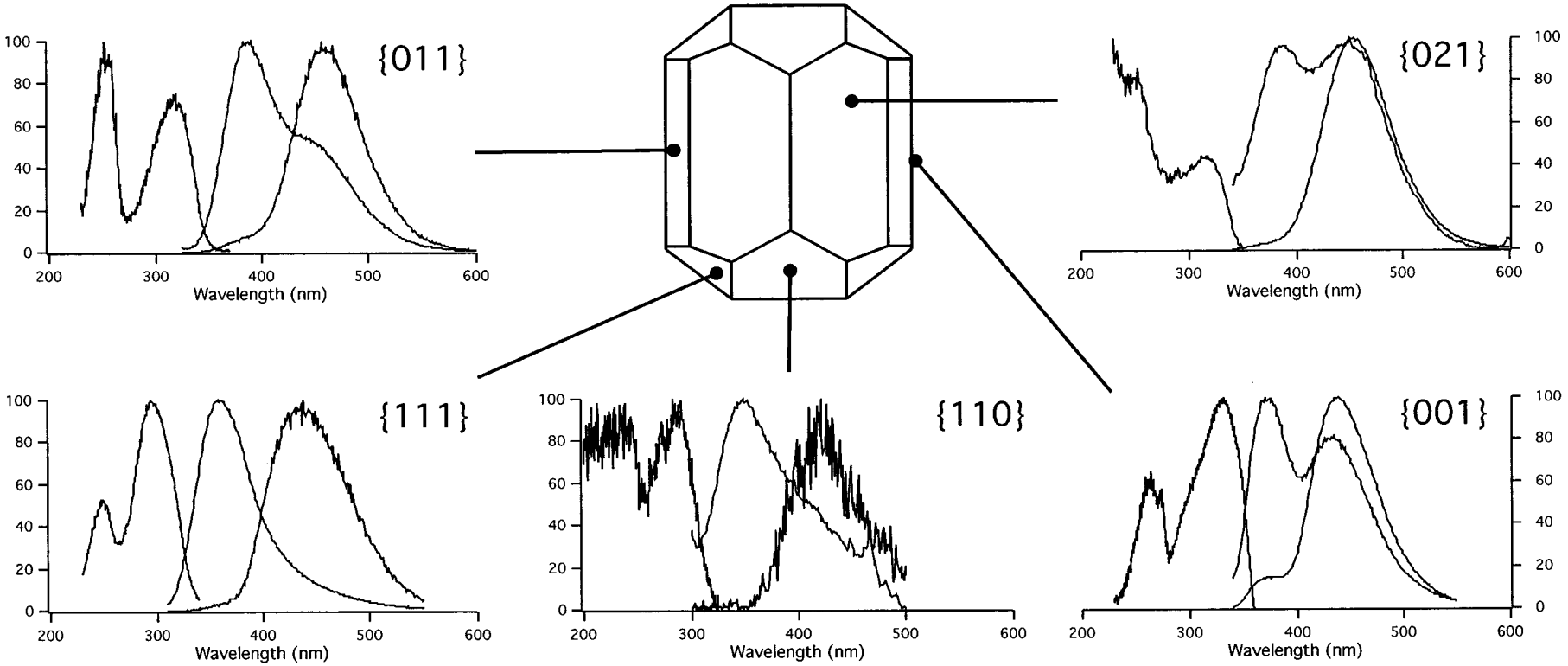

Figure 7. Multiluminescence of **3o** in single crystals of K_2SO_4. Excitation, fluorescence and phosphorescence spectra are shown for light collected from each of the developed facets. The ordinate is normalized intensity.

TABLE 1. Spectral Data for 3o[a]

		fluorescence		phosphorescence	
environment	excitation λ (nm)	λ (nm)	τ (ns) [a_i] (χ^2)	λ (nm)	τ (s) (χ^2)
K_2SO_4 {021}	250, 317	388	4.8 (1.05)	454	0.4 (1.13)
K_2SO_4 {011}	255, 319	387	4.7 (1.06)	460	0.5 (1.01)
K_2SO_4 {001}	263, 331	372	3.6 (1.14)	438	0.9 (0.95)
K_2SO_4 {111}	250, 296	360	1.6 (0.96)	438	0.1 (1.23)
K_2SO_4 {110}	240(br), 288	350	1.2 [0.93], 5.5 [0.04]; (1.05)	424	
Rb_2SO_4 {001}	258, 329	375	1.1 (0.919)	432	0.3 (1.34)
H_2O (1.0 M HCl)	221, 265, 272, 296(w)	363	1.6 (1.04)		
H_2O	260, 277, 317	363	1.7 (0.99)		
H_2O (1.0 M KOH)	244, 296	366(w); 449	6.7 (1.00)		
$C_6H_5SO_3^-$ (H_2O)	229(w), 261, 270	279, 287	0.9 (1.02)		

[a] br, broad; w, weak; a_i, pre-exponential factor.

and 5×10^3:1, respectively), the extra sulfonate may actually hinder encapsulation.

In some crystals of K_2SO_4/**1** or K_2SO_4/**2**, {110} sectors also phosphoresced, albeit with higher energy and lesser intensity than their respective {021} sectors (Figure 6). This second phosphorescent species was indicated in the EPR spectra as a minor component with a larger ZFS. The spectra of this species ($|D| = 0.0947$ cm^{-1}, $|E| = 0.0122$ cm^{-1}) are quite like those of naphthalene ($|D| = 0.1003$ cm^{-1}, $|E| = 0.0137$ cm^{-1})[33] indicating that the $-NH_2$ group is electronically uncoupled from the π system, presumably by rotation about the C−N bond (Figure 5c and 6). Wavelength selective excitation ($\lambda_{ex} > 360$ nm) showed that only the major species were observed for **1** and **2**. Separation of the sectors and dissolution of each in water revealed a single solution species. Thus we may conclude that growing K_2SO_4 crystals selected, spatially localized, and froze nearly equienergetic solution conformations.

2. Multiluminescence and Inhomogeneous Broadening. With the advent of single molecule spectroscopy,[34] it has been shown that individual luminophores can serve as reporters of subtly different local environments in crystals.[35] The dissection of ensemble-averaged spectral bands promises to reveal the nature of inhomogeneous broadening. However, it is very difficult to provide structural explanations for relative energy shifts of chromophores in single-crystal matrixes. Salted benzenes could well contribute to a structural understanding of inhomogeneous broadening in that different photophysical properties may be associated with specific surface structures.

To approach the conformational analysis and computation of spectroscopic properties such as those presented in the previous section more quantitatively, we used the benzene derivative, **3o**, a molecule small enough for cost-effective *ab initio* molecular orbital analysis, instead of **2** (Figure 1).

K_2SO_4/**3o** showed an astonishing range of luminescence energies that were correlated with the sector structure of the host (Figure 7). The spectrum from {110} was most easily distinguished from the other four by its substantially higher excitation, fluorescence, and phosphorescence energies. This mimicked the behavior of K_2SO_4/**1** and K_2SO_4/**2** whose high-energy spectra were also associated with {110}. The spectra from the {001}, {021}, and {111} faces were similar, yet nevertheless showed distinct energies, luminescence lifetimes, and ratios of steady-state fluorescence and phosphorescence (Table 1).[36]

The fluorescence energies for the five sectors are arranged in decreasing order in Table 1. The more energetic the emission, the shorter the lifetime. Such a correlation is suggestive of the fact that the differences among the molecules in the sectors are a consequence of a progressive rotation of the $-NH_2$ lone electron pair out of conjugation with the π system.[37] Only two

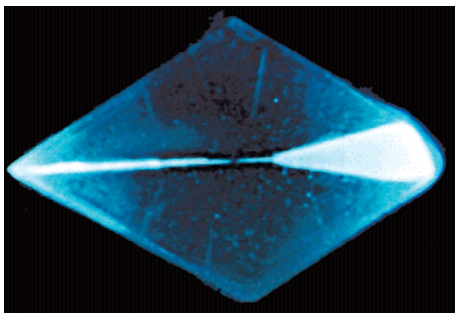

Figure 8. Photo of crystal of K_2SO_4/**3o** (14 × 10 × 5 mm) viewed along *a* illustrating the large preference for incorporation on {001} as compared with {0*k*1} where $k = 1$, 2, and 3. Horizontal direction is [001] and vertical direction is [010].

conformers were isolated in K_2SO_4/**1** and K_2SO_4/**2**, but with K_2SO_4/**3o** there is evidence of four. The phosphorescence energies follow the trend for fluorescence for K_2SO_4/**3o**, but the phosphorescence lifetimes are not correlated with the presumed variation in conformation. Even though the phosphorescence lifetime is thought to have a $\cos\theta\sin\theta$ dependence on the $-NH_2$ rotational angle,[38] nonradiative components are typically more sensitive to the environment.[39]

Protonated **3o** with a pK_a of 4.6 is a minor solution species in saturated K_2SO_4 solutions but could conceivably be enriched in the crystal.[40] To rule out this possibility we compared the photophysical properties of **3o** in a 1 M HCl solution and an aqueous solution of benzenesulfonate, with **3o** in the various sectors of K_2SO_4. The excitation spectrum of the protonated species resembled those of benzenesulfonate and benzene, but not that of any sector containing **3o**. On heating crystals to 300 °C the differences in the photophysical properties of the various sectors gradually diminished, suggesting an annealing of non-equilibrium conformations or environments.

The most abundant **3o** species in K_2SO_4 is associated with the {001} sector (Figure 8). Single-crystal EPR indicated that **3o** is oriented in the *bc* plane similar to **1** and **2** in the {021} sectors of K_2SO_4/**1** and K_2SO_4/**2**, respectively. Accordingly, the representation surface for the **D** tensor of **3o**, except for being slightly larger, resembles the orientation of the tensor for **1** with respect to the crystal axes (Figure 9).[41] The ZFS parameters of the major species in K_2SO_4/**1** and K_2SO_4/**2** are smaller than expected, but for K_2SO_4/**3o** ($|D| = 0.0727(4)$ cm^{-1}, $|E| = 0.0217(4)$ cm^{-1}) they are much smaller than expected.[42] Compare the parameters for 2-aminonaphthalene ($|D| = 0.0913$ cm^{-1}, $|E| = 0.0130$ cm^{-1}),[43] and aniline ($|D| = 0.1229$ cm^{-1}, $|E| = 0.0352$ cm^{-1}).[44] Since it is well-known that ZFS parameters are sensitive to local electric fields[45] we can assume that our guests, in an ionic salt (K_2SO_4), must experience these in abundance; this is a subject of ongoing analysis.

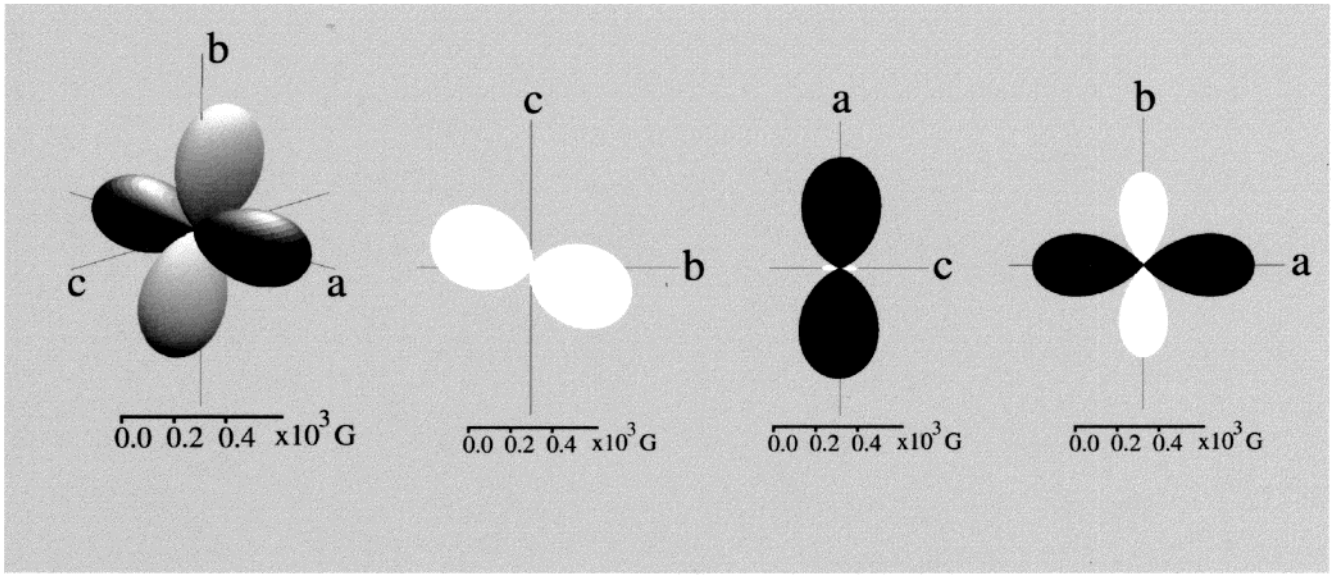

Figure 9. Representation surface and principal cross sections for the **D** tensor of K_2SO_4/**3o**. The black and white lobes indicate opposite sign of the zfs.

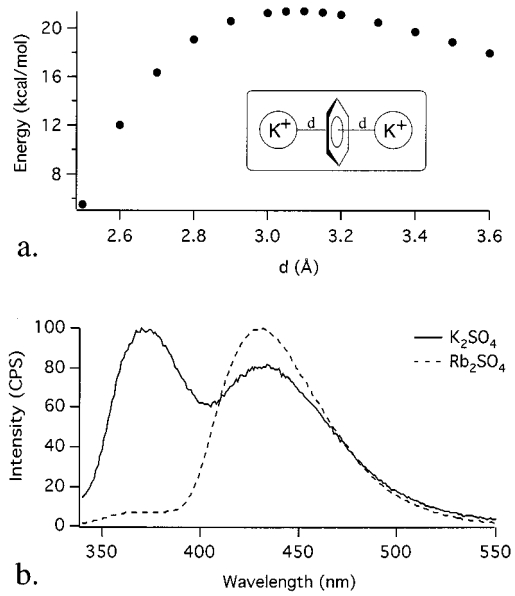

Figure 10. (a) Binding energies of D_{6h} $C_6H_6K_2^{2+}$ computed as a function of $d_{K^+-K^+}$. (b) Comparison of fluorescence and phosphorescence yields from crystals of K_2SO_4 and Rb_2SO_4 containing **3o** in the {001} growth sectors.

Hydrogen bonding of the triplet excited state with H_2O molecules in the first coordination sphere of the guest in the lattice may also be responsible for perturbing the triplet wave function.[46] For example, for **1** in an absolute ethanol glass the ZFS parameters were $|D| = 0.0985$ cm^{-1} and $|E| = 0.0140$ cm^{-1} whereas in a wet ethanol glass we saw an additional species with much smaller values $|D| = 0.0752$ cm^{-1} and $|E| = 0.0196$ cm^{-1}.[27]

Dougherty has proposed the cation$-\pi$ interaction as an important and general noncovalent binding force in a wide range of systems.[47] Calculated values for the $K^+\cdots C_6H_6$ complex were between 15 and 19 kcal/mol.[48] As benzenes in K_2SO_4 crystals cannot avoid cations we calculated the stabilization energy for the 6-fold symmetric "inverse sandwich" $K^+\cdots C_6H_6\cdots K^+$ (Figure 10a) as a function of $K^+\cdots K^+$ distance. The minimum energy structure, with a stabilization energy of 21.4 kcal/mol, had D_{6h} symmetry and a $K^+\cdots K^+$ separation of 6.2 Å, quite close to the *a* lattice constant of 5.8 Å in K_2SO_4. Since K^+ ions in K_2SO_4 are translationally related along the *a* lattice direction at a distance corresponding to a stabilization energy of 20.4 kcal/mol, these K^+ ions might sandwich the arenes in an orientation perpendicular to the *a* axis, consistent with the single-crystal EPR results that placed **3o** in the *bc* plane. The reduced energy for the "inverse sandwich" is due to the repulsive interactions when the $K^+\cdots K^+$ separation is decreased from the minimum energy configuration.

Experimental evidence for cation$-\pi$ interactions comes from the observation that **3o** in the {001} sectors of K_2SO_4 showed a much smaller phosphorescence/fluorescence yield than **3o** in the {001} sectors of isomorphous Rb_2SO_4 (Figure 10b). Moreover, the lifetime of the phosphorescence from K_2SO_4/**3o** crystals was 0.9 s whereas from Rb_2SO_4/**3o** it was 0.3 s. These observations presemably are the result of a heavy atom induced spin$-$orbit coupling. It has been demonstrated by optical detection of magnetic resonance that intersystem crossing rates for aromatic compounds are only influenced by heavy atoms if they are interacting with the face of the π system.[49]

Growing K_2SO_4 crystals also incorporate the constitutional isomers **3m** and **3p** as well as benzenesulfonate but to a lesser extent than **3o**. Not surprisingly, K_2SO_4 crystals also incorporate the toluene derivative **4** in abundance demonstrating that the presence and conformation of the *ortho*$-NH_2$ substituent plays a critical role in recognition of the crystal and in determining the photophysical properties of the guests. This proposition is currently being investigated with *o*-phenolsulfonate.

o-Sulfonated anilines are conformationally subtle as the interplay between H$\cdots$O interactions is balanced by the electronic effect of lone electron pair conjugation. Two minimum energy conformations, **3o-I** and **3o-III** (Figure 11[50]), were found at the RHF/6-31G* level of theory. **3o-I** had the lone electron pair of nitrogen in conjugation with the π system with a single H-bond between $-NH_2$ and $-SO_3^-$, while **3o-III** had the lone pair in the plane of the benzene ring permitting two H-bonds between the *ortho*-substitutents. At the RHF/6-31+G* level, minima **I** and **II** were located. The differences among **I**, **II**, and **III** are most succinctly expressed by the $HNCC_S$ torsion angles which are $-22°/-152°$, $4°/138°$, and $-53°/53°$, respectively (C_S indicates carbon attached to the $-SO_3^-$ group). At the B3LYP/6-31G* level **I** and **II** were minima while **III** was

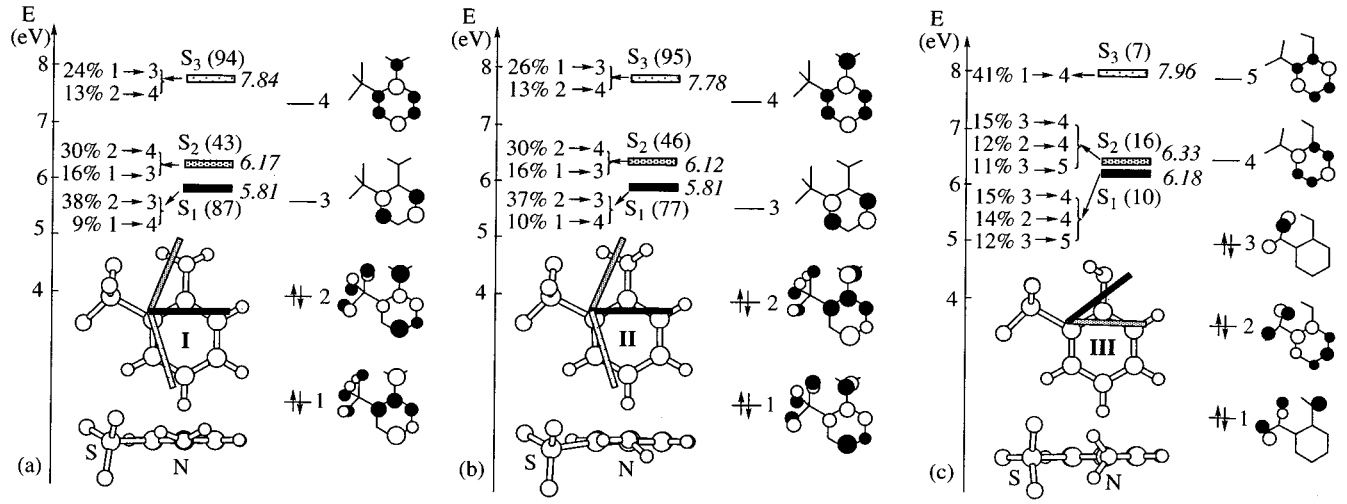

Figure 11. Results of CIS/6-31G* calculations on **3o-I**, **II**, and **III**. The leftmost column shows the composition of the excited states in terms of one-electron excitations involving the MOs shown on the right. Calculated relative oscillator strengths are in parentheses, and vertical excitation energies are in italics. The style of the presentation was adapted from ref 47.

TABLE 2. Relative Energies (kcal/mol) of 3o Conformations

conformation	RHF/6-31G*	RHF/6-31+G*	B3LYP/6-31G*
I	0.000	0.000	0.000
II	N/A	0.506	0.952
III	0.351	N/A	2.779 (TS)

a transition state for the C−N bond rotation. Regardless of the level of theory, the differences in energy among the **3o** structures were within 3 kcal/mol. Crystal forces may affect the C−N bond rotation and cause substantial changes in the photophysical properties.[51] Cazeau-Dubroca showed that even aniline in solution adopts both in- and out-of-plane conformations and displays solvent and temperature-dependent dual luminescence.[52]

The excitation energies for the first three lowest lying singlet excited states of each conformation of **3o** were calculated using the configuration interaction singles method (CIS/6-31G*).[53] Figure 11 shows conformations **I**, **II**, and **III**, along with the ETDMs for B3LYP optimized geometries.[54] For **I**, it is seen that the lowest energy transition is polarized perpendicular to the C−N axis while the next transition is almost parallel to this axis. These results are similar to those of aniline.[55] The energetics and molecular orbitals of **I** and **II** are very similar yet quite different from **III**. Thus, it appears that conformation is not alone in determining the great spectral variability of K_2SO_4/**3o**. Perturbations of the conformations by the salt matrix and/or environmental differences must also be significant.

B. Intrasectoral Zoning. *1. Luminescent Probes of Crystal Growth Mechanisms.* Biologically minded chemists have long resorted to luminescent label or probe molecules to illuminate the specificity of noncovalent interactions.[56] Crystal growth from solution, like cellular processes, is also governed by the specificity of noncovalent interactions, and as such we might expect that such probe molecules might be equally revealing. Here, we show how light emitting benzene derivatives have revealed specific aspects of crystal growth.

The luminescence from individual K_2SO_4/**3o** was not always uniform; we saw striking blue bands associated with {021} (Figure 12). As this crystal also has macrosteps that are visible to the eye it is plain to see that the stripes correspond to the slowly advancing steps of the growth spirals; **3o** only recognized the steps growing toward {001} rather than those growing toward {010}.[57] Thus, not only did **3o** select among the growing faces of K_2SO_4, it further chose particular emergent structures on a given face. Researchers have previously observed that composition in a crystal can vary because of the selective recognition of emergent dislocations by elemental ions.[58,59] This type of compositional heterogeneity or *intrasectoral* zoning, here extended to organic impurities, can be used to image growing surface structures.

The interpretations of such patterns of luminescence, whose cause can be traced to molecular recognition events on the growing crystal surfaces, require a knowledge of structures of steps and kinks. We are working to marry images of topography and local luminescence obtained by force and optical scanning probe microscopies.[60] But, even in the absence of a nanoscale description, a great deal about these structures can be obtained quickly using relatively inexpensive differential interference contrast (DIC) and fluorescence microscopies.[61]

Even though, to the best of our knowledge, growth hillocks on K_2SO_4 surfaces have never before been directly observed, Buckley described the "rounded and uneven" {021} surfaces,[18c] which Tutton referred to as "striated and distorted.",[62,63]

To preserve surface structures, crystals were pulled through a layer of hexanes sitting atop the growth solution.[64] The DIC image in Figure 13a and the idealized representation in Figure 14 illustrates typical growth spirals on the (021) surface of a K_2SO_4/**3o** mixed crystal. The steps advancing in the direction of the (010) face (vicinal face ***A***) are polygonized and have velocities several orders of magnitude greater than those bunching toward the (001) face (vicinal face ***B***). Following the step train away from the dislocation outcrop of the macrospiral smaller, singular growth spirals emerge from the steps that eventually become overgrown by the rapidly advancing macrospiral (Figure 13b). Near the hillock core, the step risers in vicinal face ***A*** indexed optically as (031), whereas the step risers in ***B*** indexed as (011). The flats were always (021). The straight-sloped ***A*** vicinal face is composed of alternating (021) and (031) surfaces while the curving ***B*** vicinal face adsorbs, orients, and overgrows **3o**.

The selective staining of the ***B*** vicinal face must be related to the mechanism of incorporation of **3o** within this surface. Preliminary evidence indicated that the planes of **3o** and **1** are both perpendicular to the *a* axis of the K_2SO_4 crystal. If a sulfonate−sulfate substitution model is invoked for **3o** as was for **1**, the selective staining demonstrates the importance of the $-NH_2$ group in recognizing the surfaces: compare (011), (021),

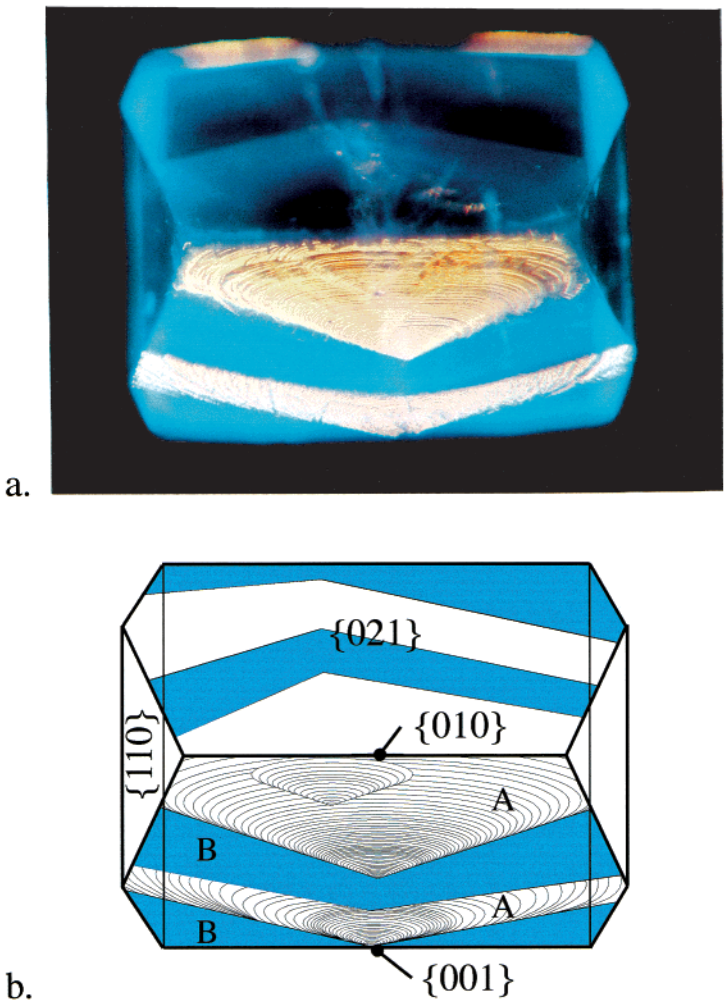

Figure 12. (a) K_2SO_4/**3o** illuminated with short wavelength UV light and a visible flashlight reflected off of the lower facet. Lateral dimension is 1 cm. Growth spirals partition the {021} face into {031}-like and {011}−like vicinal zones marked *A* and *B*, respectively. (b) Idealized representation of the crystal. Positions of a face in the {010} and {001} families are indicated for reference had they been developed.

(031), and (001) surfaces in Figure 5a in relation to the $-NH_2$ group of **1**. Faces whose inclinations are suited to interact with both the $-SO_3$ and the $-NH_2$ groups, {001} and {011}, incorporate **3o**, while others, {031} and {010}, do not (Figure 5).

2. Determination of Absolute Growth Directions. Prior to the recent determination of absolute configuration by inspection using scanned probe microscopies,[65] only a very small number of ways of assigning absolute stereochemistry have been invented.[66] The interpretation by Addadi *et al*. of additive induced habit changes in terms of the stereospecific interactions at crystal interfaces is most relevant for our discussion.[67] An especially pertinent example is the identification by Weissbuch et al. of enantiotopic faces of α-glycine bipyramids by habit modification and selective etching in the presence of resolved amino acid additives.[68] Here, we assign the absolute growth directions of an achiral salt crystal using growth additives in a manner conceptually analogous to the aforementioned example, although our assignment will be made not from changes in crystal form and topography but rather from patterns of light emitted by benzene derivatives in the crystals.

Our observation that room-temperature phosphorescence (RTP) is a common attribute of salted aromatics led us to study crystals of NaOAc (Ac = $-OC(O)CH_3$)·$3H_2O$ (*C*2/*c*)[69] grown in the presence of *p*-aminobenzoate (**5p**), a model system for studying SSRTP. We prepared large single crystals of NaOAc·$3H_2O$/**5p** so that we could deduce a mechanism for mixed crystal growth from the anisotropy of the optical properties. NaOAc·$3H_2O$ crystals with luminescent ($\lambda_p = 413$ nm, $\tau_p = 1.6$ s) {001} growth sectors were grown at room temperature from saturated aqueous salt solutions containing *p*-aminobenzoic acid (1×10^{-2} M). The average ratio of moles of NaOAc to moles of **5p** in these crystals was ∼2000. The long axis transition moment[70] of **5p** included within the NaOAc·$3H_2O$ crystal was determined from the luminescence intensity as a function of excitation polarization, and was consistent with **5p** approaching the surface carboxylate first, and substituting for a carboxylate group of an acetate ion.[71]

Given this carboxylate-carboxylate substitution model we selected a crystalline matrix for RTP that would orient **5p** predictably and promote phosphorescence via external heavy atom induced spin-orbit coupling.[72] $Ba(OAc)_2$ ($I4_1/a$, $Z = 32$ with two independent molecules in the unit cell)[73] crystals grown from aqueous **5p** solutions contained the guest in the {011}, {012}, and {013} growth sectors. The luminescence, almost exclusively phosphorescence ($\lambda_p = 427$ nm) with a predictably shorter lifetime ($\tau_p = 5.4$ ms) than that of NaOAc·$3H_2O$/**5p** crystals, was polarized orthogonally in adjacent sectors according to the host symmetry and was consistent with a carboxylate-carboxylate substitution model involving acetate ions emerging from the {01*l*} faces.

$Ba(OAc)_2$ crystals are achiral (point group C_{2h}) and dense

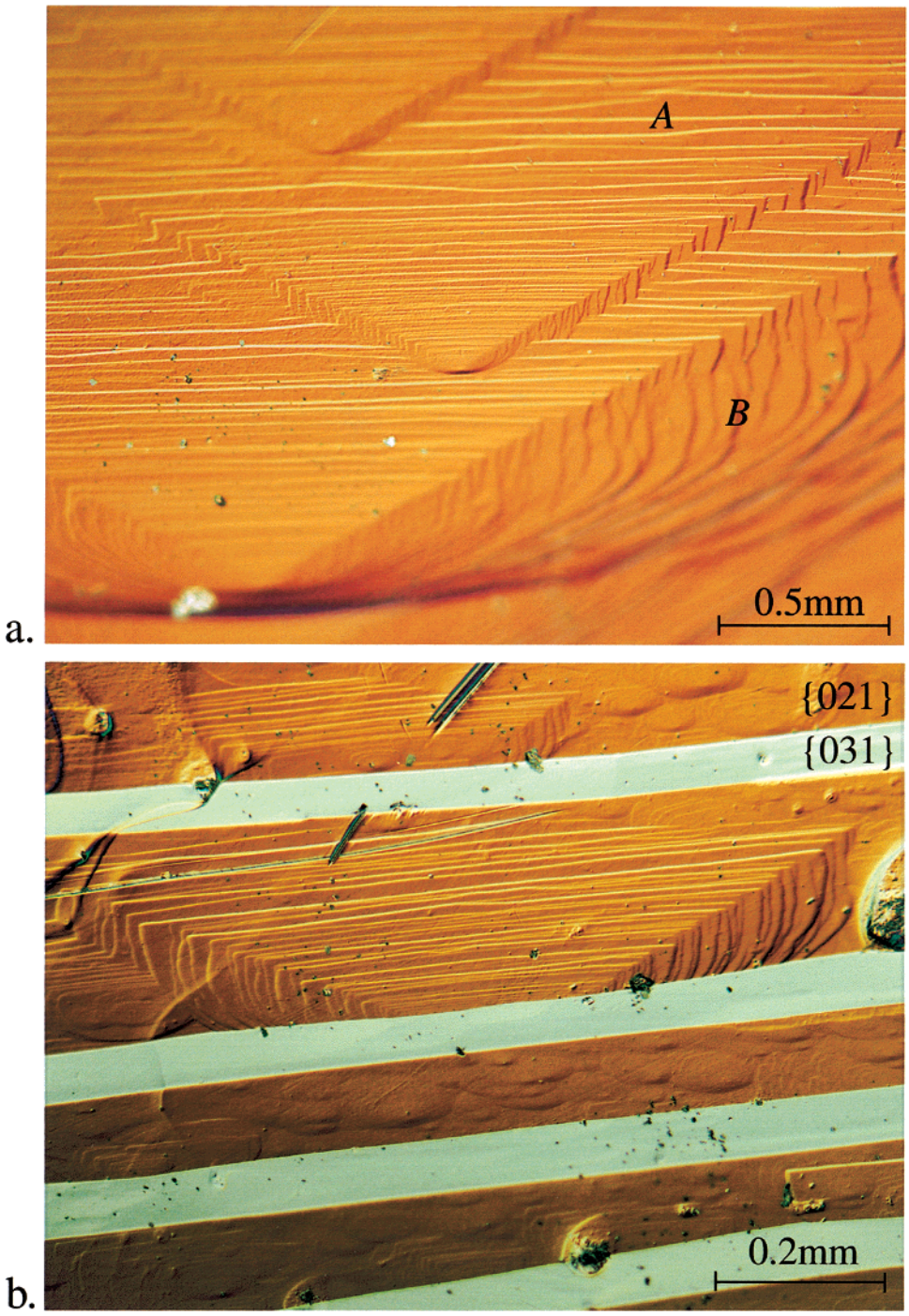

Figure 13. Differential interference contrast images of {021} surface structures of K_2SO_4/**3o** illustrating characteristic macroscopic, cooperating growth hillocks.

(2.47 g/mL). They invariably fall to the bottom of dishes on their {001} faces and therefore grow in the $+c$ or the enantiomorphous $-c$ direction with equal probability. However, when crystals grown in the presence of **5m** or **5p** were irradiated with UV light, we observed luminescent pinwheel-like structures within the crystals, "spinning" clockwise or counterclockwise (Figure 15). This observation instantly partitioned the crystals into two sets having grown in one direction or the other, a Pasteur-like resolution and determination of absolute hand using luminescence.

Furthermore, the pinwheels signaled the presence of reentrant angles during early, rapid growth, that bisected the lateral edges (Figure 16a,b). The resulting concave surfaces provide a natural explanation for why the pinwheel blades do not correspond to growth sectors, causing compositional variation, intrasectoral zoning, within {01*l*}. This variation undoubtedly arises because of the differential recognition of the sixteen translationally inequivalent acetates in the unit cell that have different presentations on each {01*l*} surface (Figure 16c). They must be recognized selectively, but which acetates do the molecules of **5** prefer? If we assume that carboxylate-carboxylate substitution is the driving force for mixed crystal formation, with respect to (011), we can limit our discussion to include only four of the translationally inequivalent acetates, labeled green in Figure 16d, positioned for substitution by **5** with methyl groups sticking out of the face. The blue acetates are pointing into this face

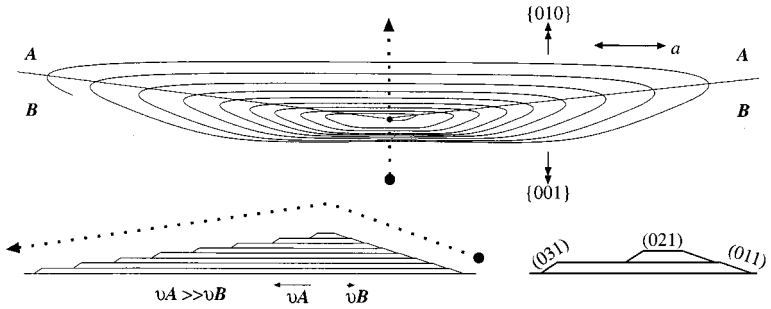

Figure 14. Idealized representation of the growth spirals on the (021) surface of K_2SO_4/**3o**. The advancement velocity of the steps (υ) in the *A* vicinal face (υ_A), is much greater than that in *B* (υ_B). The (011), (031), and (021) indicies of the risers and step, respectively, were determined by reflection from a crystal, mounted on a spindle stage, viewed through the differential interference contrast microscope.

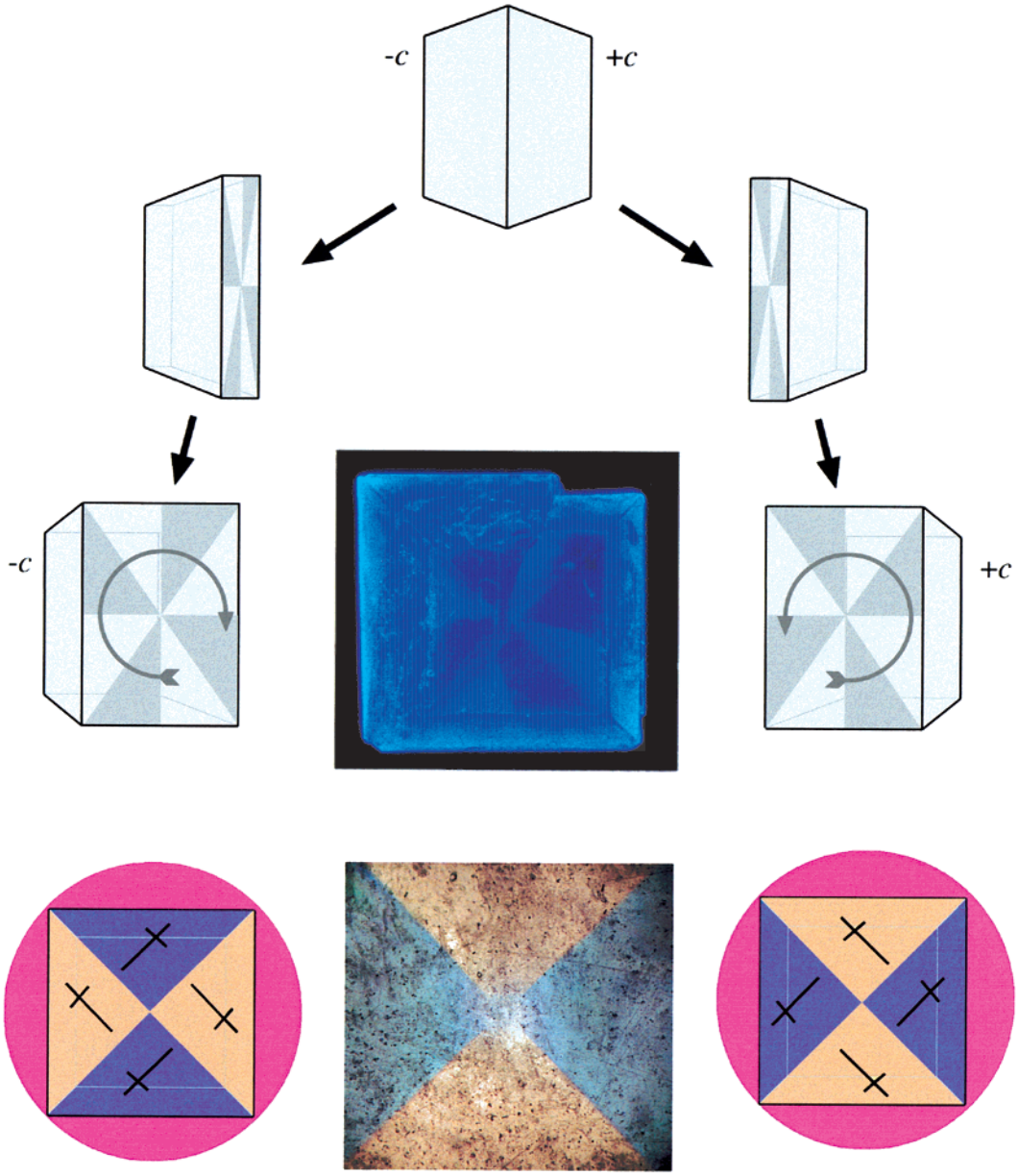

Figure 15. Schematic representation of enantiomorphous pinwheels and their relationship to absolute *c* direction. Center: Photograph of a crystal of $Ba(OAc)_2$/**5p**, viewed along [001], showing luminescent pinwheel. Bottom: Photograph of the interference colors resulting from the linear birefringence in crossed polarized light with a first-order red compensator. Schematic representations are correlated with directions of pinwheels. Crossed black bars represent slow (long) and fast (short) crystallographic vibration directions.

rather than out of it, while their mirror symmetric orange and red partners are pointing down, a poor configuration for recognition of a crystal growing in the $+c$ direction.

The four remaining acetates are sensibly distinguished once the high-index faces appear (Figure 16d). In any half-sector of (011), now only one pair of acetates (**III** and **IV**) has their

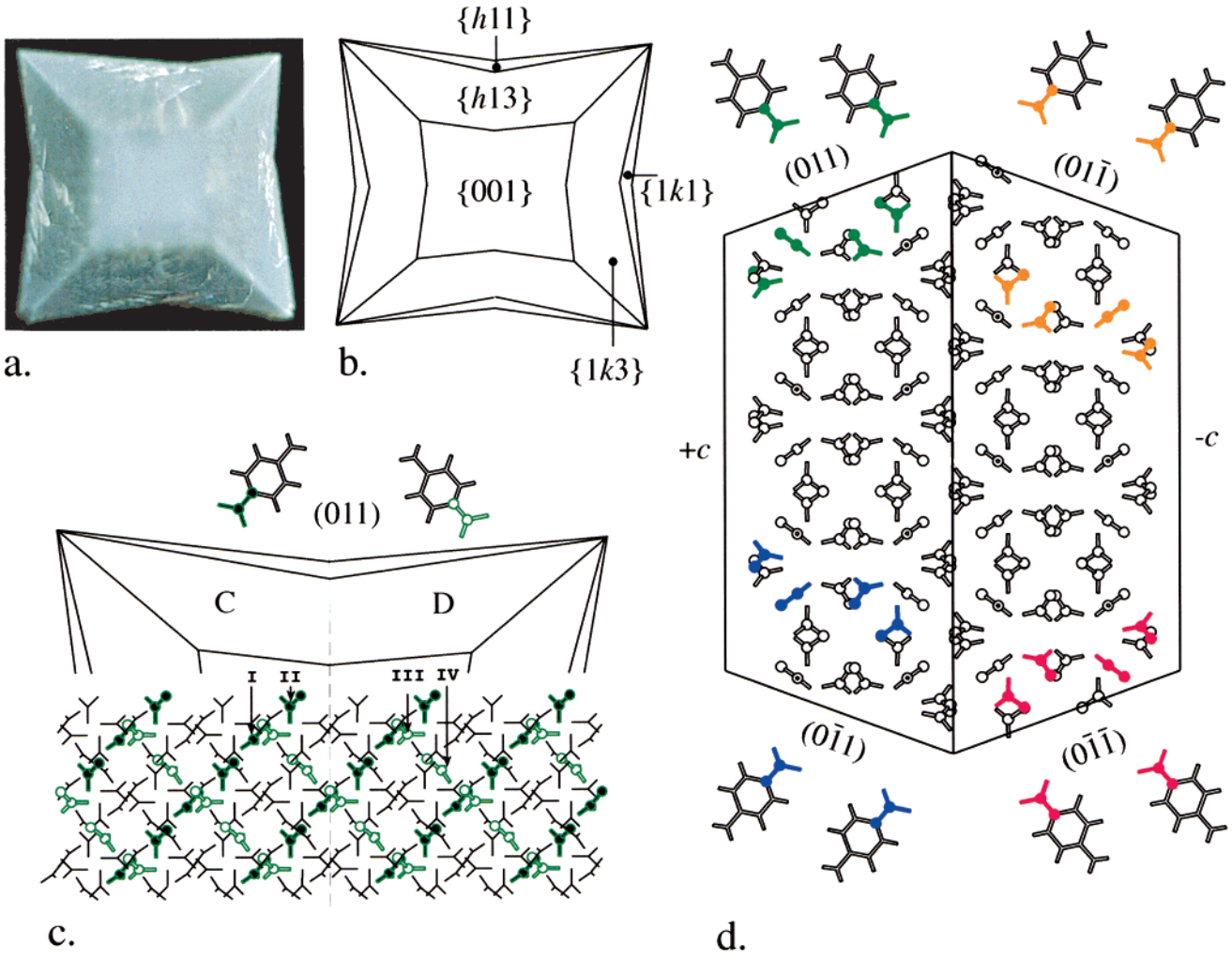

Figure 16. (a) Photo of $Ba(OAc)_2$/**5m** pinwheel crystal with (b) an idealized representation of the habit. (c) Relative orientation of the $Ba(OAc)_2$ crystal structure and habit. Due to the high index faces, the black acetates (**I**, **II**) are preferred in region **C**, whereas the colorless acetates (**III**, **IV**) are preferred in region **D**. The substitution of **III** and **IV**, in preference to **I** and **II**, by **5** causes the observed pinwheel phenomenon (d) Green, orange, blue, and red acetates are responsible for incorporation of **5** in (011), (01$\bar{1}$), (0$\bar{1}$1), and (0$\bar{1}\bar{1}$), respectively. Ba^{2+} ions and hydrogens have been omitted for clarity.

$C-CH_3$ vectors pointing out of the *D* surface. Given the directionality of the observed pinwheel we can then propose that this pair, **III** and **IV**, is recognized in preference to the others.

Polarized excitation spectra for mixed crystals of $Ba(OAc)_2$/**5p** that do not have interpenetrating faces nor pinwheels, support the idea that the four acetates, **I**, **II**, **III**, and **IV** were recognized equally. Luminescence intensities collected normal to (100) and (001) as a function of excitation polarization indicated that the molecules of **5p**, with long axis polarization, were aligned along the body diagonals of the crystals, exactly like the four acetates **I**, **II**, **III**, and **IV**.

Clearly the incorporation of **5m** or **5p** into $Ba(OAc)_2$ affects a reduction of symmetry. While there is virtually no way of observing this by X-ray scattering, the effect was easily seen in crossed polarized light (Figure 15).[74] As viewed through a first-order red quartz compensator, the blue and yellow interference colors seen in adjacent sectors indicated that the once uniaxial host is now composed of biaxial growth sectors arranged around an improper 4-fold axis. This desymmetrization mechanism is quite like those in other pseudo tetragonal mixed or disordered crystals such as 11-bromoundecanoylperoxide or 1,5-dichloro-2,3-dinitrobenzene studied by McBride and coworkers.[75] Naturally, the linear birefringence correlated with the hand of the pinwheel (Figure 15) but was not sensitive to whatever effect gave rise to the pinwheels. In other words, we could not discern pinwheels of birefringence. One can argue that the pinwheels must be present in images of both the luminescence and linear birefringence. Studies using birefringence imaging systems that are more sensitive than the eye are currently in progress.[76] As with many examples of anomalous linear birefringence the cause of the distorted optical indicatrix was not easily assigned.[77] However, the disposition of the fast and slow axes in the biaxial sectors is rational if we assume the carboxylate-carboxylate substitution mechanism and that the biggest change in polarizability occurs in the mixed crystal along the long axis of **5p**.

$Ba(OAc)_2$ also encapsulated **5o**, but not **3o**, **3m**, or **3p**. Moreover, K_2SO_4 was indifferent to **5o**, **5m**, and **5p**. The affinity of benzoates for acetates and sulfonates for sulfates suggests that the matching of anions and anionic functionalities are especially important in mixed crystal growth in these cases.

III. Single Crystal Matrix Isolation Unconstrained by Isomorphism

Mitscherlich's principle of isomorphism[78] requires that if you want to put X into a crystal made from Y, X and Y must have

the same size and shape. Metallurgists have quantified this intuitive concept in Hume-Rothery's rule.[79] Goldschmidt[80] and Kitaigorodsky[81] extended it to minerals and molecular crystals, respectively. In a review of the history of the development of the principle of isomorphism,[82] Freund wisely cautioned against adopting fixed criteria since all pairs of substances possess to some extent the property of forming mixed crystals. Nevertheless, the Hume-Rothery, Goldschmidt, and Kitaigorodsky rules have been widely adopted while consequently discouraging the use of single crystals as matrixes, especially for complex organic molecules.[83] Michl and Thulstrup pointed out that the use of single-crystal matrix isolation is rare because of the difficulty of finding isomorphous host-guest pairs.[84]

Classic examples of single-crystal matrix isolation are the demonstration that the phosphorescent state was paramagnetic with crystals of durene (1,2,4,5-tetramethylbenzene) containing naphthalene,[85] and the realization of single-molecule detection with *p*-terphenyl crystals containing pentacene.[86,87] The McClure and Moerner groups, respectively, relied on the fact that host and guest molecules were similar in size and shape permitting the formation of an "oriented gas." Notable departures from the constraint of isomorphism on single-crystal matrix isolation are the Shpol'skii mixed crystals, polyaromatic hydrocarbons in *n*-alkane crystals;[88] here the isomorphism is one-dimensional only. Needless to say, single *n*-octane crystals are quite difficult to prepare and even more difficult to manipulate compared with salt polyhedra.

Simple ionic crystals containing benzene derivatives facilitates the mutual study of both components. In freezing out and spatially localizing guest molecules in subtly different conformations, the host exercises constraints that allow spectroscopic investigation of parts of potential energy surfaces that are otherwise not obtainable.[89] In recognizing host surfaces and steps differentially the guests serve to illuminate crystal growth mechanisms. The wealth of information obtained by orienting analytes in crystals and then discriminating variations in properties in different parts of a given crystal is both a help and a hindrance. Nevertheless, large well-faceted, transparent salt crystals should be considered matrixes for the study of organic compounds. Lest the reader get the impression that only small benzene and naphthalene derivatives can be accommodated by salt crystals, we have salted phthalocyanines, giant benzene derivatives with a great variety of optical applications,[90] in K_2SO_4 and KH_2PO_4.[91]

During our work with dyed crystals, encouraged by evidence from the older crystallographic literature,[92] and from contemporary fields of biomineralization[93] and MALDI mass spectrometry,[94] we have abandoned the principle of isomorphism[95] and prepared many common salt, sugar, and aromatic crystals containing a wide variety of oriented guests. We hope that the examples illustrated herein, among others, will encourage others to skirt thermodynamic intuition and to exploit the driving force of supersaturated solutions far from equilibrium to design a greater range of ill-matched hosts and guests for purposes yet undiscovered.

IV. Experimental Section

Chemicals were reagent grade, purchased from Aldrich unless otherwise indicated and included the following: 2-amino-1,5-naphthalene disulfonic acid (Pflatz-Bauer), 2-amino-1-naphthalene sulfonic acid (TCI America), potassium sulfate (Mallinckrodt), *p*-aminobenzoic acid, *m*-aminobenzoic acid, *o*-aminobenzoic acid (Matheson Coleman & Bell), *p*-aminobenzene sulfonic acid, *m*-aminobenzene sulfonic acid, *o*-aminobenzene sulfonic acid, 4-aminotoluene-3-sulfonic acid, barium acetate, and sodium acetate (Fischer). Dionized water for crystallizations was distilled using a Corning Mega-Pure System MP-1.

Typical growth solutions contained >25 mg guest per gram of host. Guest concentrations in crystals were determined from the absorbance of dissolved crystals. Typical mixed crystals were grown in 5−7 days by the slow evaporation from dishes inside an undisturbed cabinet. This *laissez-faire* approach to crystal growth proved superior to crystals grown from seeds or in constant temperature water baths. Crystals were indexed optically using a STOE Darmstadt optical goniometer, and by X-ray diffraction with Nonius KappaCCD Diffractometer.

Ultraviolet absorption spectra were recorded with a Hitachi U-2000 spectrophotometer controlled with SpectraCalc software (Galactic Industries). Fluorescence spectra were recorded with a SPEX FluoroMax-2 fluorimeter, and phosphorescence spectra were obtained with a phosphoroscope fashioned from a soup can. For those samples with a visible excitation, spectra were collected from polished thin sections of crystals on an Olympus IMT-2 inverted microscope equipped with a 1 m bifurcated, randomized fiber optic bundle, MI02EF microscope interface, Model 1950 Fiber Optic Platform (Instruments S. A.), dichroic filters, and a dichroic mirror (Chromatek). For other crystals, anisotropy was measured in the FluoroMax-2 cavity fitted with Glan-Thompson prisms. Sector specific luminescence spectra were obtained by painting all other faces with a black Sharpie marker.

Linear birefringence was studied with an Olympus BH2 polarizing microscope and a Berek compensator. Differential interference contrast images were obtained with a Leica DMLM reflected light microscope and captured with a Diagnostic Instruments SPOT digital camera.

Luminescence lifetimes were determined by measuring the decay of the emission with a Photon Technologies International (PTI) Timemaster fluorescence lifetime spectrometer equipped with a gated detector for long-lived phosphorescence. A frequency doubled N_2 pumped dye laser was used to excite the samples. Data analysis was performed with PTI's TimeMaster Pro Version 1.2.

Electron Paramagnetic Resonance (EPR) spectra were recorded on a Bruker ESP 300 EPR spectrometer (X-band) with a 100 kHz Zeeman modulation, operating at 10−20 mW. An Oriel mercury-xenon high-pressure arc lamp (Model 666021) operating at 200−300 W was used to photolyze the samples. The light was filtered through water (path length 9 cm) and a Corning CSO-56 long pass filter (1.73 mm, >260 nm). Crystals were mounted on 20 cm long Suprasil quartz rods (o.d. = 4 mm, i.d. = 2.6 mm) with epoxy and oriented in the cavity with a Teflon and brass goniometer fashioned to the dimensions of the spectrometer. Orienting the crystals on the quartz rods was facilitated by their size (10−100 mm^3) and by the fact that they were well formed with sharp crystallographic edges.

Computations on benzene derivatives were carried out with Gaussian 98.[96] Ground-state geometries were optimized using the Hartree-Fock SCF method (RHF/6-31G* and RHF/6-31+G*) as well as by Becke's three-parameter hybrid density functional-HF method with the Lee-Yang-Parr correlation functional (B3LYP/6-31+G*). Stationary points were characterized by frequency analysis. For excited-state calculations, the Franck-Condon excitation energies for the three lowest lying singlet excited states and the ETDMs were determined using configuration interaction taking only single substitutions into account (CIS/6-31G*) with the B3LYP/6-31G* optimized geometry. Adiabatic transitions were calculated from the energy

difference between the minima on the ground and excited states. Cation−π calculations were carried out at the B3LYP level of theory with the LANL2DZ basis set that uses the Los Alamos effective core potential for potassium.[97]

Acknowledgment. We thank the National Science Foundation (Grants CHE-9457374 and CHE-9727372), the University of Washington Royalty Research Fund, and the donors of the American Chemical Society-Petroleum Research Fund (Grant 30688-AC6) for financial support. We are indebted to Bruce Robinson and Colin Mailer for the use of the Bruker EMX spectrometer. We are grateful to John Heutink and Lon Buck for assistance in building phosphoroscopes, Scott Lovell for indexing crystals, and Michael Mombourquette for programming advice.

Supporting Information Available: Fractional coordinates of model of major species in K_2SO_4/**1** from Figure 5a,b. Fractional coordinates of model of minor species in K_2SO_4/**1** from Figure 5c. EPR field positions for K_2SO_4/**3o**. Calculated fits of EPR data. Nondiagonal tensor used to generate surfaces in Figure 9. Absolute energies (hartrees), cartesian coordinates (angstroms), vibrational frequencies (cm^{-1}), and intensities (km/mol) of **3o** conformations. This material is available free of charge via the Internet at http://pubs.acs.org.

References and Notes

(1) Kirkor, E.; Gebicki, J.; Phillips, D. R.; Michl, J. *J. Am. Chem. Soc*. **1986**, *108*, 7106−7107. Also see Böttcher, H.; Hertz, O.; Fritz, T. *Chem. Phys. Lett.* **1988**, *148*, 237−240. Böttcher, H.; Hertz, O.; Fox, M. A. *Chem. Phys. Lett*. **1989**, *160*, 121−128.

(2) Kirkor, E. S.; Maloney, V. M.; Michl, J. *J. Am. Chem. Soc*. **1990**, *112*, 148−151. Conditions have subsequently been adjusted to overcome the problems of aggregation. Michl, J. Private communication.

(3) Kirkor, E. S.; David, D. E.; Michl, J. *J. Am. Chem. Soc.* **1990**, *112*, 139−147.

(4) Sénarmont, H. *C. R. Séances Acad. Sci*. **1854**, *38*, 101−105; *Ann. Phys. Chem*. **1854**, *167*, 491−494.

(5) For a complete history of dyeing crystals, see: Kahr, B. *Chem. Rev*. manuscript to be submitted. Abbreviated histories appear in refs 7, 8, 14, 21c, and 21d.

(6) Prior to our recent research, spectroscopic studies of dye inclusion crystals have been limited to three qualitative observations: (a) Buckley, H. E. *Mem. Proc. Manchester Lit. Philos. Soc.* **1951**, *92*, 77−123. (b) Hartmann, H. In *Zur Physik und Chemie der Kristallphosphore*; Akademie Verlag: Berlin, 1960. (c) Slavnova, E. N. In *Growth of Crystals (Rost Kristallov): Reports at the first Conference on Crystal Growth 5−10 March 1956;* Consultants Bureau: New York, 1958; 117−125. (Slavnova, E. N. In *Growth of Crystals* Shubnikov, A. V., Sheftal', N. N., Eds.; Consultants Bureau: New York, 1959; Vol. 2, pp 32−35.)

(7) Kahr, B.; Jang, S.-H.; Subramony, J. A.; Kelley, M. P.; Bastin, L. D. *Adv. Mater*. **1996**, *8*, 941−944.

(8) Kahr, B.; Chow, J.; Peterson, M. L. *J. Chem. Educ.* **1994**, *71*, 584−586. Kahr, B.; Kelley, M. P. In *Supramolecular Stereochemistry*; Siegel, J. S., Ed.; Kluwer: Dortrecht, 1995; pp 203−221.

(9) Rifani, M.; Yin, Y.-Y.; Elliott, D. S.; Jay, M. J.; Jang, S.-H.; Kelley, M. P.; Bastin, L.; Kahr, B. *J. Am. Chem. Soc.* **1995**, *117*, 7572−7573.

(10) Kahr, B.; Lovell, S.; Subramony, J. A. *Chirality* **1998**, *10*, 66−77.

(11) Vetter, W. M.; Dudley, M.; Kahr, B. in *National Synchrotron Light Source Report*; Hurlburt, S. L., Lazarz, M. L., Eds.; Brookhaven National Laboratories: Upton, New York, 1993. Kelley, M. P.; Kahr, B.; Dudley, M. In *National Synchrotron Light Source Report*; Rothman, E. Z., Ed.; Brookhaven National Laboratories: Upton, New York, 1994.

(12) Sedarous, S.; Subramony, J. A.; Kahr, B. *Ferroelectrics* **1997**, *191*, 301−306. Subramony, J. A.; Jang, S.-H.; Kahr, B. *Ferroelectrics* **1997**, *191*, 292−300.

(13) Mitchell, C. A.; Gurney, R. W.; Jang, S.-H., Kahr, B. *J. Am. Chem. Soc*. **1998**, *120*, 9726−9727.

(14) Mitchell, C. A.; Lovell, S.; Thomas, K.; Savickas, P.; Kahr, B. *Angew. Chem., Int. Ed. Engl.* **1996**, *35*, 1021−1023. Lovell, S.; Subramony, P.; Kahr, B. *J. Am. Chem. Soc*. **1999**, *121*, 7020−7025.

(15) Chmielewski, J.; Lewis, J. J.; Lovell, S.; Zutshi, R.; Savickas, P.; Mitchell, C. A.; Subramony, J. A.; Kahr, B. *J. Am. Chem. Soc*. **1997**, *119*, 10565−10566. Kurimoto, M.; Subramony, P.; Gurney, R. W.; Lovell, S.; Chmielewski, J.; Kahr, B. *J. Am. Chem. Soc.* **1999**, *121*, 6952−6953.

(16) Frondel reported having oriented dyes in alkali halide crystals, but we have had difficulty preparing well defined, mixed crystals according to his procedures. See: Frondel, C. *Am. Mineral*. **1940**, *25*, 91−110.

(17) For previous examples of aromatic compounds in K_2SO_4 crystals, see: Retgers, J. W. *Z. Phys. Chem*. **1893**, *12*, 583−622. Buckley, H. E. *Z. Kristallogr*. **1934**, *88*, 181−184; **1934**, *88*, 248−255; *Angew. Chem*. **1941**, *51*/*52*, 527−536. Rigterink, M. D.; France, W. G.; *J. Phys. Chem*. **1938**, *42*, 1079−1088. Neuhaus, A. *Z. Kristallogr*. **1942**, *104*, 197−224; Whetstone, J. *Discuss. Faraday Soc*. **1954**, *16*, 132−140.

(18) Groth, P. *Chemische Krystallographie*, Wilhelm Engelmann: Leipzig, 1908; Vol. 2, pp 337−340

(19) Wyckoff, R. G. *Crystal Structures*; Wiley-Interscience: New York, 1965; Vol. 3, p 95. Also see: Ojima, K.; Nishihata, Y.; Sawada, A. *Acta Crystallogr., Sect. B* **1995**, *51*, 287−293.

(20) Paquette, J.; Ward, W. B.; Reeder, R. J. In *Carbonate Microfabrics*; Rezak, R., Lavoie, D., Ed.; Springer-Verlag: 1993; pp 243−252; Rakovan, J.; Reeder, R. J. *Am. Mineral*. **1994**, *79*, 892−903.

(21) For example, see: (a) Lehman, O. *Ann. Phys. Chem*. **1894**, *51*, 47−76. Gaubert, P. *Bull. Soc. Min. Fr*. **1900**, *23*, 211−221. (b) Neuhaus, A. *Z. Kristallogr*. **1943**, *105*, 161−219. (c) Buckley, H. E. *Crystal Growth*; John Wiley: New York, 1951. (d) France, W. G. *Colloid Symp. Annu*. **1930**, *7*, 57−87.

(22) Vaida, M.; Shimon, L. J. W.; Weisinger-Lewin, Y.; Frolow, F.; Lahav, M.; Leiserowitz, L.; McMullan, R. K. *Science*, **1988**, *241*, 1475−1479. Vaida, M.; Weissbuch, I.; Lahav, M.; Leiserowitz, L. *Isr. J. Chem*. **1992**, *32*, 15−21. Weissbuch, I.; Popovitz-Biro, R.; Lahav, M.; Leiserowitz, L. *Acta Crystallogr*. **1995**, *B51*, 115−148. Also see: Aizenberg, J.; Hanson, J.; Koetzle, T. F.; Leiserowitz, L.; Weiner, S.; Addadi, L. *Chem. Eur. J*. **1995**, *1*, 414−422.

(23) Paynter, R. A.; Wellons, S. L.; Winefordner, J. D. *Anal. Chem*. **1974**, *46*, 736−738.

(24) Vo-Dinh, T. *Room-Temperature Phosphorimetry for Chemical Analysis*; John Wiley: New York, 1984. Hurtubise, R. J. *Phosphorimetry: Theory, Instrumentaion and Applications*; VCH: New York, 1990. There have been >180 original contributions to this literature since 1998.

(25) Gunshefski, M.; Santana, J. J.; Stephenson, J.; Winefordner, J. D. *Appl. Spectrosc. Rev*. **1992**, *27*, 143−192. Hurtubise, R. J. *Anal. Chim. Acta* **1997**, *351*, 1−22.

(26) Weil, J. A. *EPR−NMR*; University of Saskatchewan: Saskatoon, 1993. Also see: Rinneberg, H.; Weil, J. A. *J. Chem. Phys*. **1972**, *56*, 2019−2028.

(27) Smaller, B.; Avery, E. C.; Remko, J. R. *Mol. Phys*. **1971**, *21*, 999−1013.

(28) Ridley, J.; Zerner, M. C. *Theor. Chim. Acta*, **1973**, *32*, 111−134; *Theor. Chim. Acta* **1976**, *42*, 223−236.

(29) Hilinski, E. F. Ph.D. Dissertation, Yale University, 1982.

(30) Mitchell, C. A. Ph.D. Dissertation, Purdue University, 1998.

(31) Rohl et al. have illustrated the role of phosphonate−sulfate substitution in the crystal inhibition of barite ($BaSO_4$). See: Rohl, A. L.; Gay, D. H.; Davey, R. J.; Catlow, C. R. A. *J. Am. Chem. Soc*. **1996**, *118*, 642−648. and references therein.

(32) Kelley, M. P.; Janssens, B.; Kahr, B.; Vetter, W. M. *J. Am. Chem. Soc*. **1994**, *116*, 5519−5520. Bastin, L. D.; Kahr, B. Unpublished results.

(33) Hutchison, C. A.; Magnum, B. W. *J. Chem. Phys*. **1961**, *34*, 908−922. Hornig, A. W.; Hyde, J. S. *Mol. Phys*. **1963**, *6*, 33−41.

(34) Moerner, W. E.; Orrit, M. *Science* **1999**, *283*, 1670−1676. Weiss, S. *Science* **1999**, *283*, 1676−1683.

(35) For example, see: Skinner, J. L.; Moerner, W. E. *J. Phys. Chem*. **1996**, *100*, 13251−13262. Moerner, W. E. *Acc. Chem. Res*. **1996**, *29*, 563−571.

(36) For a review of environmental effects on the photophysical properties of aniline, see: Sarkar, S. K.; Kastha, G. S. *Spectrochim. Acta A*, **1992**, *48A*, 1611−1624.

(37) Köhler, G. *J. Photochem*. **1987**, *38*, 217−238. Shimamori, H.; Sato, A. *J. Phys. Chem*. **1994**, *98*, 13481−13485.

(38) Kasha, M.; Rawls, H. *Photochem. Photobiol.* **1968**, *7*, 561−569. Lim, E. C.; Chakrabarti, S. K. *J. Chem. Phys.* **1967**, *47*, 4726−4730.

(39) Hatch, G. F.; Erlitz, M. D.; Nieman, G. C. In *Molecular Luminescence*; Lim, E. C., Ed.; W. A. Benjamin: New York, 1969; pp 21−38; Chaudhuri, N. K.; El-Sayed, M. A. *J. Chem. Phys.* **1965**, *43*, 1423−1424; *J. Chem. Phys.* **1966**, *44*, 3728−3732. El-Sayed, M. A. *Chem. Rev.* **1965**, 199−241.

(40) Moskvin, A. F.; Doktorova, L. I.; Kazankina, É. I.; Reznikova, I. A.; Belyaev, V. A. *Zh. Obshch. Khim*. **1979**, *49*, 669−672; *J. Gen. Chem. USSR* **1979**, *49*, 581−584.

(41) Plotted using *WinTensor*, Version 1. Kaminsky, W. 1998.

(42) Nagaoka, S.; Harrigan, E. T.; Noda, M.; Hirota, N.; Higuchi, J. *Bull. Chem. Soc. Jpn*. **1986**, *59*, 355−361.

(43) Veeman, W. S.; Van den Hoek, W. J. *Mol. Phys*. **1967**, *13*, 197−198.

(44) Van Noort, H. M.; Vergragt, P. J.; Herbich, J.; van der Waals, J. H. *Chem. Phys. Lett*. **1980**, *71*, 5−11.

(45) Clarke, R. H. ed. *Triplet State ODMR Spectroscopy*; John Wiley and Sons: New York, 1982.

(46) Cazeau-Dubroca, C.; Nouchi, G.; Ben Brahim, M.; Pesquer, M.; Gorse, D.; Cazeau, P. *J. Photochem. Photobiol. A. Chem*. **1994**, *80*, 125−133; Cazeau-Dubroca, C.; Ait Lyazidi, S. A.; Cambou, P.; Peirigua, A.; Cazeau, P.; Pesquer, M. *J. Phys. Chem*. **1989**, *93*, 2347−2358. Cazeau-Dubroca, C.; Ait Lyazidi, S.; Nouchi, G.; Peirigua, A.; Cazeau, Ph. *Nouv. J. Chim*. **1986**, *10*, 337−343. Also see: Herbich, J.; Grabowski, Z. D.; Wojtowicz, H.; Golankiewicz, K. *J. Phys. Chem*. **1989**, *93*, 3439−3444.

(47) Ma, J. C.; Dougherty, D. A. *Chem. Rev.* **1997**, *97*, 1303−1324.

(48) Kumpf, R. A.; Dougherty, D. A *Science*, **1993**, *261*, 1708−1710. Caldwell, J. W.; Kollman, P. A. *J. Am. Chem. Soc.* **1995**, *117*, 4177−4178.

(49) Ghosh, S.; Petrin, M.; Maki, A. H.; Sousa, L. R. *J. Chem. Phys.* **1987**, *87*, 4315−4323; Maki, A. H. *Methods Enzymol*. **1995**, *246*, 610−638.

(50) See: Zhu, Z.; Bally, T.; Stracener, L. L.; McMahon, R. J. *J. Am. Chem. Soc*. **1999**, *121*, 2863−2874.

(51) Ghoshal et al. have shown that n−π* transitions of guest molecules in molecular crystals are quite sensitive to phase transformations, see: Ghoshal, S. K.; Sarkar, S. K.; Kastha, G. S. *Mol. Cryst. Liq. Cryst*. **1983**, *91*, 1−24.

(52) Dubroca, C. *Chem. Phys. Lett*. **1972**, *15*, 207−210; Dubroca, C.; Lozano, P. **1974**, *24*, 49−54.

(53) Foresman, J. B.; Head-Gordon, M.; Pople, J. A.; Frisch, M. J. *J. Phys. Chem*. **1992**, *96*, 135−149.

(54) For the suitability of these methods for determining conformational effects on benzene transition moments see: Kroemer, R. T.; Liedl, K. R.; Dickinson, J. A.; Robertson, E. G.; Simons, J. P.; Borst, D. R.; Pratt, D. W. *J. Am. Chem. Soc*. **1998**, *120*, 12573−12582. Bulliard, C.; Allan, M.; Wirtz, G.; Haselbach, E.; Zachariasse, K. A.; Detzer, N.; Grimme, S. *J. Phys. Chem. A.* **1999**, *103*, 7766−7772.

(55) Cazeau-Dubroca, C. *J. Lumin*. **1984**, *29*, 349−364.

(56) Haugland, R. P. *Handbook of Fluorescent Probes and Research Chemicals*; Molecular Probes: Eugene, OR, 1996.

(57) For the orientation of additives by crystallographic steps, see: Bonafede, S. J.; Ward, M. D. *J. Am. Chem. Soc*. **1995**, *117*, 7853−7861. Carter, P. W.; Ward, M. D. *J. Am. Chem. Soc*. **1993**, *115*, 11521−11535.

(58) See for example: Paquette, J.; Reeder, R. J. *Geochim. Cosmochim. Acta* **1995**, *59*, 735−749. Paquette, J.; Reeder, R. J. *Geology* **1990**, *18*, 1244−1247. Allen, F. M.; Buseck, P. R. *Am. Mineral*. **1988**, *73*, 568−584.

(59) (a) Zaitseva and co-workers have used dyes that we provided to selectively recognize the slopes of hillocks on the {101} faces of KDP crystals. See: Zaitseva, N.; Carman, L.; Smolsky, I.; Torres, R.; Yan, M. *J. Cryst. Growth* **1999**, *204*, 512−524. (b) Vetter, W. M.; Dudley, M.; Wong, T.-F.; Fredrich, J. T. *Mater. Res. Soc. Symp. Proc*. **1996**, *406*, 561−566. (c) Meguro, K.; Koishi, M.; Takada, S. *J. Colloid. Interface Sci.* **1967**, *23*, 294−297.

(60) Gurney, R. W. Unpublished results.

(61) Pluta, M. *Advanced Light Microscopy, Specialized Methods*; Elsevier: New York, 1989; Vol. 2.

(62) Tutton, A. E. *J. Chem. Soc.* **1894**, 628−717. Bunn, C. W.; Emmett, H. *Discuss. Faraday Soc*. **1949**, *5*, 119−132.

(63) Bennema and co-workers predicted using Hartman-Perdok theory that the {021} surfaces would be of lesser morphological importance. See: Vogels, L. J. P.; Verheijen, M. A.; Bennema, P. *J. Cryst. Growth* **1991**, *110*, 604−616.

(64) Enckevort, W. J. P. v. *Prog. Cryst. Growth Charact.* **1984**, *9*, 1−50.

(65) Fang, H. B.; Giancarlo, L. C.; Flynn, G. W. *J. Phys. Chem. B* **1998**, *102*, 7311−7315. De Feyter, S.; Gesquiere, A.; Grim, P. C. M.; De Schryver, F. C.; Valiyaveettil, S.; Meiners, C.; Sieffert, M.; Mullen, K. *Langmuir* **1999**, *15*, 2817−2822.

(66) Bijvoet, J. M.; Peerdeman, A. F.; van Bommel, A. J. *Nature* **1951**, *168*, 271−272. Paul, I. C.; Curtin, D. Y. *Organic Solid State Chemistry*; Elsevier: Amsterdam, 1987; p 331. Walba, D. M.; Razavi, H. A.; Clark, N. A.; Parmar, D. S. *J. Am. Chem. Soc*. **1988**, *110*, 8686−8691. Wang, J. L.; Lahav, M.; Leiserowitz, L. *Angew. Chem., Int. Ed. Engl*. **1991**, *30*, 696−698.

(67) Addadi, L.; Berkovitch-Yellin, Z.; Weissbuch, I.; van Mil, J.; Shimon, L. J. W.; Lahav, M.; Leiserowitz, L. *Angew. Chem., Int. Ed. Engl*. **1985**, *24*, 466−485. Addadi, L.; Berkovitch-Yellin, Z.; Weissbuch, I.; Lahav, M.; Leiserowitz, L. *Topics in Stereochemistry*; Eliel, E., Willen, S. H., Allinger, N. L., Eds.; **1986**, *16*, 1−85.

(68) Weissbuch, I.; Lahav, M.; Leiserowitz, L.; Meredith, G. R.; Vanherzeele, H. *Chem. Mater*. **1989**, *1*, 114−118.

(69) Efremov, V. A.; Endeladze, N. O.; Agre, V. M.; Trunov, V. K. *Zh. Strukt. Khim.* **1986**, *27*, 177−180.

(70) Halpern, A. M.; Ramachandran, B. R. *Photochem. Photobiol.* **1995**, *62*, 686−691.

(71) Carboxylate−carboxylate substitution has been shown to be important in a variety of mixed amino acid crystallizations. See ref 22.

(72) Kasha, M. *J. Chem. Phys*. **1952**, *20*, 71−74. Seybold, P. G.; White, W. *Anal. Chem.* **1975**, *47*, 1199−1200. White, W.; Seybold, P. G. *J. Phys. Chem.* **1977**, *81*, 2035−2040.

(73) Gautier-Luneau, I.; Mosset, A. *J. Solid State Chem*. **1988**, *73*, 473−479.

(74) Hartshorne, N. H.; Stuart, A. *Crystals and the Polarizing Microscope*, 4th ed.; Edward Arnold: London, 1970.

(75) McBride, J. M.; Bertman, S. *Angew. Chem., Int. Ed. Engl*. **1989**, *28*, 330−333. Kahr, B.; McBride, J. M.; *Angew. Chem., Int. Ed. Engl*. **1992**, *31*, 1−26.

(76) Glazer, A. M.; Lewis, J. G.; Kaminsky, W. *Proc. R. Soc. London A* **1996**, *452*, 2751−2765.

(77) Crundwell, G.; Gopalan, P.; Bakulin, A.; Peterson, M. L.; Kahr, B. *Acta Crystallogr. Sect. B* **1997**, *B53*, 189−202. Crundwell, G. A.; Cowans, B.; Hopkins, J.; Grutzner, J.; Kahr, B. *J. Solid State Chem*. **1999**, *145*, 327−335.

(78) Melhado, E. M. *Hist. Stud. Phys. Sci*. **1980**, *11*, 87−123.

(79) Hume-Rothery, W. *The Structure of Metals and Alloys*; Institute of Metals and Alloys: London, 1936.

(80) Goldschmidt, V. M. *Skr. Nor. Vidensk. Akad. Oslo* **1926**, 1 N2.

(81) Kitaigorodsky, A. I. *Mixed Crystals*; Springer-Verlag: Berlin, 1984.

(82) Freund, I. *The Study of Chemical Composition. An Account of Its Method and Historical Development*; Dover: New York, 1968.

(83) McClure, D. S. *Electronic Spectra of Molecules and Ions in Crystals*; Academic Press: New York, 1959; pp 24−47. Dicker, A. I. M.; Johnson, L. W.; Völker, S.; van der Waals, J. H. *Chem. Phys. Lett.* **1983**, *100*, 8−14.

(84) Michl, J.; Thulstrup, E. W. *Spectroscopy with Polarized Light: Solute Alignment by Photoselection in Liquid Crystals, Polymers, and Membranes*; VCH: New York, 1995.

(85) McClure, D. S. *J. Chem. Phys*. **1954**, *22*, 1668−1675. Also see: Hutchison, C. A. In *The Triplet State*; Zahlan, A. B., Ed.; University Press: Cambridge, 1967; pp 63−100.

(86) Moerner, W. E.; Kador, L. *Phys. Rev. Lett*. **1989**, *62*, 2535−2538.

(87) For a favorite example, see: Hollingsworth, M. D.; McBride, J. M. *J. Am. Chem. Soc*. **1985**, *107*, 1792−1793.

(88) Nurmukhametov, R. N. *Russ. Chem. Rev*. **1969**, *38*, 180−193.

(89) McBride, J. M.; Segmuller, B. E.; Hollingsworth, M. D.; Mills, D. E.; Weber, B. A. *Science* **1986**, *234*, 830−835.

(90) Leznoff, C. C., Lever, A. B. P., Eds. *Phthalocyanines: Properties and Applications*, VCH: New York, 1989; Vol. 2.

(91) Subramony, J. A. Ph.D. Dissertation, Purdue University, 1999. Gurney, R. W.; Bastin, L. D. Unpublished results.

(92) For other examples, see: Johnsen, A. N. *Jahrestag. Mineral. Geol. Pal*. **1903**, *II*, 93−138. Seifert, H. *Fort. Mineral. Kristallogr. Petrogr*. **1935**, 103−181; *Fort. Mineral. Kristallogr. Petrog.* **1936**, 324−455; *Fort. Mineral. Kristallogr. Petrog.* **1937**, 185−488.

(93) For example, see: Addadi, L. *Chimia* **1999**, *53*, 156−162. Aizenberg, J.; Hanson, J.; Koetzle, T. F.; Weiner, S.; Addadi, L. *J. Am. Chem. Soc*. **1997**, *119*, 881−886. Weiner, S.; Addadi, L. *J. Mater. Chem.* **1997**, *7*, 689−702.

(94) Fournier, I.; Beavis, R. C.; Blais, J. C.; Tabet, J. C.; Bolbach, G. *Int. J. Mass Spectrom. Ion Proc*. **1997**, *169/170*, 19−29. Kampmeier, J.; Dreisewerd, K.; Schürenberg, M.; Strupat, K. *Int. J. Mass Spectrom. Ion Proc*. **1997**, *169/170*, 31−41.

(95) For an earilier contemporary example, see ref 68. Even pentacene is not restricted to *p*-terphenyl as host. See: Ong, J.-L.; Sloop, D. J.; Lin, T.-S. *J. Phys. Chem.* **1993**, *97*, 7833−7838. For a wholly inorganic example, dicyanoargenate in KCl, see: Omary, M. A.; Patterson, H. H. *J. Am. Chem. Soc*. **1998**, *120*, 7696−7705. Omary, M. A.; Hall, D. R.; Shankle, G. E.; Siemiarczuk, A.; Patterson, H. H. *J. Phys. Chem. B*, **1999**, *103*, 3845−3853.

(96) Frisch, M. J.; Trucks, G. W.; Schlegel, H. B.; Scuseria, G. E.; Robb, M. A.; Chessemen, J. R.; Zakrzewski, V. G.; Montgomery, J. A.; Stratmann, R. E.; Burant, J. C.; Dapprich, S.; Millam, J. M.; Daniels, A. D.; Kudin, K. N.; Strain, M. C.; Farkas, O.; Tomasi, J.; Barone, V.; Cossi, M.; Cammi, R.; Mennucci, B.; Pomelli, C.; Adamo, C.; Clifford, S.; Ochteriski, J.; Petersson, G. A.; Ayala, P. Y.; Cui, Q.; Morokuma, K.; Malick, D. K.; Rabuck, A. D.; Raghavachari, K.; Foresman, J. B.; Cioslowski, J.; Ortiz, J. V.; Stefanov, B. B.; Liu, G.; Liashenko, A.; Piskorz, P., Komaromi, I.; Gomperts, R.; Martin, R. L.; Fox, D. J.; Ketih, T., Al-Laham, M. A.; Peng, C. Y.; Nanayakkara, A.; Gonzalez, C.; Challacombe, M.; Gill, P. M. W.; Johnson, B. G.; Chen, W.; Wong, M. W.; Andres, J. L.; Head-Gordon, M.; Replogle, E. S.; Pople, J. A. *Gaussian 98*, Revision A.6; Gaussian, Inc.: Pittsburgh, PA, 1998.

(97) Hay, P. J.; Wadt, W. R. *J. Chem. Phys.* **1985**, *82*, 299−310.